

NASA TECHNICAL NOTE



NASA TN D-2242

C.1

LOAN COPY: 1
AFWL (M)
KIRTLAND AF

0154841



TECH LIBRARY KAFB, NM

NASA TN D-2242

HIGH-SPEED PHOTOGRAPHIC
INVESTIGATION OF THE
FORMATION OF DETONATION WAVES
IN A STOICHIOMETRIC
HYDROGEN-OXYGEN MIXTURE

*by James A. Laughrey, Loren E. Bollinger,
and Rudolph Edse*

Prepared under Grant No. NsG-44-60 by
OHIO STATE UNIVERSITY
Columbus, Ohio
for



HIGH-SPEED PHOTOGRAPHIC INVESTIGATION
OF THE FORMATION OF DETONATION WAVES
IN A STOICHIOMETRIC HYDROGEN-OXYGEN MIXTURE
By James A. Laughrey, Loren E. Bollinger, and Rudolph Edse

Prepared under Grant No. NsG-44-60 by
OHIO STATE UNIVERSITY
Columbus, Ohio

This report was reproduced photographically
from copy supplied by the contractor.

NATIONAL AERONAUTICS AND SPACE ADMINISTRATION

For sale by the Office of Technical Services, Department of Commerce,
Washington, D. C. 20230 -- Price \$1.25

TABLE OF CONTENTS

	Page
SUMMARY	1
INTRODUCTION	3
EXPERIMENTAL EQUIPMENT	5
EXPERIMENTAL PROCEDURE	9
DISCUSSION OF RESULTS	11
CONCLUSIONS	18
REFERENCES	21
FIGURE	
1 Pictorial View of Detonation Tube	26
2 Exploded View of Detonation-Tube Window	27
3 Diagram of Shadowgraph System	28
4 Distance of Flame Front from Ignitor	29
5 Distance of Shock or Detonation Front from Ignitor	30
6 Shadowgraphs of the Formation of the Detonation Wave; Ignition at End A	31
7 Shadowgraphs of the Formation of the Detonation Wave; Ignition at End B	35

HIGH-SPEED PHOTOGRAPHIC INVESTIGATION OF THE FORMATION OF DETONATION WAVES IN A STOICHIOMETRIC HYDROGEN-OXYGEN MIXTURE

By

James A. Laughrey, Loren E. Bollinger and Rudolph Edse

SUMMARY

An experimental investigation was conducted with a high-speed, image-converter camera to elucidate the mechanism by which a detonation wave is formed in a stoichiometric mixture of hydrogen and oxygen. The initial conditions of the hydrogen-oxygen mixture were one atmosphere pressure and ambient temperature. The 7.62-cm square test section of the detonation tube used for these experiments was 167 cm long. By varying the positions of a modified shadowgraph system and the glass windows, the entire length of the test section of the tube could be covered photographically. The shadowgraph system consisted of a high-intensity, short-duration, point-source lamp, two parabolic mirrors, and a high-speed image converter camera with a Polaroid back. The effective exposure time of the phenomena under observation was about 0.4 microseconds which was determined by the duration of the light pulse from the point-source lamp. The image converter tube in the image converter camera was used mainly to prevent overexposure of the film by the afterglow of the reaction. Insufficient natural radiation made it impossible to use the camera for direct photography. The image tube could be pulsed for time intervals ranging from 0.1 to 6 microseconds and could be synchronized with the point-source lamp. Appropriate delay times could be inserted into a delay unit so that the event to be photographed could be synchronized with the exposure.

Considerable detail was obtained in the shadowgraphs of the flame, shock front, and other discontinuities present during the formation of a detonation. The entire distance from the ignitor to

the location at which the detonation wave formed was covered during this study. Immediately after ignition the flame front was shown to be laminar and dome shaped. Its propagation rate was relatively slow compared to the final detonation velocity. The flame front continually accelerated and shock waves were formed in front of it with the leading shock wave having a fairly constant velocity (approximately 690 m/sec) until just prior to the formation of the detonation wave. The shock wave was first observed approximately 33 cm from the ignitor; the separation between the flame and shock front gradually increased until a distance of 80 to 90 cm from the ignitor was reached. Then explosion-like reactions occurred immediately in front of the flame front, which caused the burning region to accelerate and coalesce with the shock front, thereby forming a detonation wave at a distance of approximately 100 to 110 cm from the ignitor.

Prior to the development of this reaction, the initially smooth flame front became wrinkled approximately 40 to 60 cm away from the ignitor; the flame front lost its domed shape and became highly irregular with the leading edge of the front located along the walls. Turbulence was observed in the gas flow between the shock wave and the flame front along the walls of the tube. The explosions just prior to detonation originate near the walls of the tube, just in front of the flame front, and cause pressure waves to propagate outward into the reacted and unreacted gas thereby reinforcing the leading shock front and sending a "retonation" wave back through the reacted gas. No autoignitions were detected in the unreacted mixture between the shock wave and the flame front.

The distance from the ignitor at which the detonation wave formed was not the same from one experiment to the next. Therefore, several experiments had to be made to obtain a complete survey of all disturbances which occurred in a particular region of the detonation tube. Some of this scatter was caused by the different window positions that had to be used. Wave interactions at the junction between the glass windows and metal side-wall generated additional shocks. Just prior to the formation of the detonation wave and after it had formed fully, transverse pressure fluctuations appeared which are similar to those observed in oscillating or spinning detonations.

Near the impact end of the tube a shock wave was observed in front of the detonation wave. Apparently a detonation wave formed in the hot mixture behind the leading shock front due to a reflection

of the leading shock at the edge of the glass window located upstream of the observed region. The detonation wave coalesced with the leading shock wave prior to impact at the end of the tube.

INTRODUCTION

The phenomena associated with the formation of a detonation wave in a combustible gaseous mixture have been studied extensively in the past decade, both theoretically and experimentally, by many investigators (e.g., see Refs. 1-48). Although the studies have been fairly extensive, there are many aspects concerning the transient formation process which have not been explained adequately from either an experimental or a theoretical viewpoint. The details of the stable detonation wave are understood much better than those of the transition mechanism from deflagration to the steady-state condition of detonation.

The flame acceleration mechanism is one phenomenon which should be understood more fully to explain the transition process. Another question which needs to be answered more adequately is how the combustion wave is established behind the shock wave of the fully-established detonation wave. One explanation is that the flame accelerates and overtakes the shock wave and another is that the combustible gases are heated to a sufficiently high temperature when passing through the shock wave so that autoignition occurs behind it and, thereby, the combustion wave is established immediately behind the shock wave. After extensive experimental study, neither of these explanations appears to be adequate. A much more detailed investigation of the various steps occurring in the unsteady transition process is needed for a complete understanding of the transition process.

Some investigators attribute the acceleration of the flame front, prior to establishment of the stable detonation wave, to turbulence in the unburnt gas mixture between the leading shock wave and the flame front. The method by which this turbulence is generated is somewhat questionable. Turbulence could be caused perhaps by particle flow in front of the flame front. This flow could become turbulent when a critical Reynolds number is attained or when the flame propagation rate reaches a certain value at which the flame front becomes turbulent. Possibly a combination of these two effects may generate the observed turbulence.

The following are the general features that are associated with the formation of a detonation wave in a combustible gaseous mixture. After ignition by some appropriate device in the tube or other type of container, the flame starts to propagate in laminar fashion at a rather slow rate. The heat released during the chemical reaction causes the temperature of the reacting gases to rise. A volume increase occurs behind the flame front. As soon as the temperature of the reacting gas begins to rise, a pressure wave is transmitted at the local sonic velocity into the unburned gas region. The next incremental temperature increase, if the continuous process is considered in a step-wise manner, generates another pressure wave which is transmitted similarly. Because the temperature of the unburned gas increases slightly after the passage of each incremental pressure wave, the local sonic velocity is increased accordingly. After an appropriate period of time has elapsed, these various pressure waves reach and reinforce the pressure wave that was propagated initially and a shock wave is formed.

This process of generating pressure waves from the flame front not only causes a shock wave to be formed and the pressure and temperature of the unreacted gas between the shock and the flame front to increase, but this unreacted gas is set into motion relative to the tube wall, thereby increasing the propagation rate of both the shock and the flame front. It appears that this process continues until a detonation wave is formed at which time the reaction propagates at a constant velocity.

Because of the relative lack of information about the details of the transition mechanism, an experimental and theoretical investigation was undertaken to elucidate the mechanism of the transient process. High-speed photography was utilized to study the process at various stages from ignition to a fully-established detonation. A modified shadowgraph system and an image converter camera were employed. Exposure times in the submicrosecond region were used to stop the motion. Photographs were obtained of the flame and shock structure which show appreciable detail in the initiation region of the detonation for a stoichiometric mixture of hydrogen and oxygen at one atmosphere initial pressure. The discussion presented herein pertains primarily to an explanation of the wave structure rather than to a detailed mathematical analysis.

EXPERIMENTAL EQUIPMENT

In this investigation of the formation of detonations in a stoichiometric hydrogen-oxygen mixture, photographic data were obtained by employing an ultra-high-speed camera system and a specially-designed detonation tube. The latter was fabricated from a solid bar of 7079 aluminum, 3 x 8 x 72 inches. The inside portion was milled out until a reaction chamber, 3 x 3 x 66 inches, was obtained. Then 1.5-inch thick aluminum side panels were added to close the open sides of the basic detonation tube.

By making suitable openings in these side panels, which could be connected to the detonation tube with studs, a total of four 20-inch long windows could be installed on both sides. When windows were not required, metal blanks could be installed. Turning the side plates allowed complete coverage of events in the tube, during a series of experiments, through opposing glass windows. The original windows were special two-inch thick, hardened, schlieren quality windows which had sides whose parallelism was held to close tolerances.

The test section of the detonation tube had a 7.62-cm square cross-section. The nominal length was 167 cm. By design, an ignitor could be positioned at either end. This feature greatly expedited the experiments. A pictorial view of the detonation tube is shown in Fig. 1.

After the first series of detonation experiments was conducted, it was found that the special windows did not stand up very well under the severe conditions which prevailed. The internal surfaces became crazed and slivers of glass broke off from the main portion. After more experiments the surfaces became so badly damaged that it was impossible to pressure-seal the windows adequately. The thermal and mechanical stresses, even at only one atmosphere initial pressure, were too great for the windows. From an ordinary stress calculation, these windows should have been quite adequate for initial pressures up to approximately seven atmospheres, including a safety factor, for a stoichiometric mixture of hydrogen and oxygen. Shock loading and intense transient temperature gradients, however, negated the steady-state, non-reacting gas mixture stress calculations.

After the large windows began to fail, adapters were made to utilize some of the smaller and thinner high-quality optical windows which were available in the laboratory. Also, some tempered, polished plate-glass windows, one-inch thick, were utilized successfully. By suitable selection of the plate glass, schlieren distortions were minimized to quite an acceptable level. These plate-glass windows withstood many experiments before they had to be replaced.

As mentioned above, the detonation tube was fabricated so that the positions of the observation windows, relative to the ignitor, could be located so as to obtain complete coverage of the test section during a series of experiments for identical initial conditions of the gas mixture. For a particular position of the windows, the observable length of the tube was 18 inches; the entire test-section height (three inches) could be seen by the camera. Each position of the windows overlapped the previous position by one inch to ensure continuous coverage. An exploded view of a particular window arrangement, showing the flanges, seals, and so forth, is illustrated in Fig. 2.

The hydrogen and oxygen gases were mixed on a flowing basis to preclude the dangers of storing a relatively large volume of a premixed, stoichiometric mixture of these gases under pressure. A description of the flow control and metering system, similar to those used for many detonation investigations at this laboratory, is given in Ref. 47. A vacuum pump was employed to remove the residual gases from the tube prior to filling it with the explosive mixture to an initial pressure of one atmosphere.

Ignition of the combustible mixture was accomplished by melting a 0.005-inch diameter bimetallic wire with a 180-volt battery. The wire consists of aluminum and palladium in intimate contact with each other. When this material is heated to the melting point of aluminum (660°C), an exothermic alloying process takes place which liberates 327 calories/gram; the temperature of the product gas near the reacting wire reaches 2200 to 2800°C .

The space available to conduct the photographic studies was rather restricted and it was necessary to utilize a folded optical arrangement as shown in Fig. 3. A modified shadow system was used which included a high-intensity point-light source, appropriate lenses and mirrors, and a high-speed image converter camera. From Fig. 3 it can be seen that two first-surface mirrors were used to fold the light beam. The 48-inch focal length, off-axis, parabolic

mirrors rendered the divergent light beam from the source parallel through the test section and then focused the beam again before entering the lens system of the image converter camera. The high-intensity lamp had a maximum energy output of 10 joules. Voltage to the storage capacitor could be varied from 10 to 20 kv and useful results could be obtained. A variable voltage power supply was employed in order to change the light-beam intensity as required for the various experiments.

Measurement of the duration of the pulse of luminous radiation from the point source showed that the pulse was approximately 400 nanoseconds wide at the half-power points. The pulse width did not change appreciably as the energy output from the storage capacitor was changed by a factor of four.

Direct photography of the combustion and detonation events was attempted with the high-speed image converter camera unit. After numerous experiments it was concluded that there was insufficient intensity from the phenomenon desired. The natural intensity of light must be quite high in order to get a usable image when the exposure time ranges from 0.1 to 6 microseconds.

The gases in the detonation tube glow for a long period of time after the primary reaction occurs. Therefore, when using the point-source lamp as a shutter, through the shuttering action of the pulsed beam, some method must be employed to limit the light input to the recording camera because of the large amount of afterglow. The image converter camera served quite well for this purpose. If the light intensity from the point source and event were too great, the exposure time of the image converter unit could be decreased to reduce the light level to an acceptable value. Ordinarily, the exposure time of the image converter camera was six microseconds. Since the pulse width of the point light source was less than one-tenth of that value, not too much difficulty was encountered in synchronizing the two shutters.

The particular image converter camera used in these studies was a relatively new type. Instead of using an image tube with a conventional electron lens, a photodiode was utilized. These diode types give greatly improved resolution over the electron-lens type; however, the resolution from the photodiode type of image converter is not as good as that which can be obtained from a high-quality, high-speed, framing camera. The versatility of the image converter camera and its much lower cost, however, make this type of camera unit quite useful for studies of this nature.

The diode gains in resolution over the electron-lens type of tube because the image is in focus for a longer period of time over the gating (shuttering) cycle. In the electron-lens type, the gating grid receives a voltage pulse to make the tube conduct for a period of time corresponding to the approximate length of the voltage pulse. Unfortunately it is not feasible to produce a very rectangular voltage pulse for these small pulse widths (in the submicrosecond region). Instead of having pulse rise-times and decay-times which are only a few nanoseconds long, the slopes are degraded, resulting in a loss in resolution. In a grid-type (electron lens) tube, the image is in focus on the anode screen only at one value of grid voltage. Therefore, when the grid gating pulse does not rise to the correct focus voltage quickly and remain there for the pulse width desired, the image resolution suffers by the amount of deviation from the correct grid voltage needed to maintain focus. In the photodiode, the anode and cathode are closely spaced; therefore, the electron stream does not have much chance to diverge and cause loss of resolution. The tube is gated with high-voltage pulses applied directly to the anode-cathode connections. To obtain a permanent record of the image displayed on the phosphor-screen anode of the photodiode, it was photographed with a secondary optical camera.

During most of the experiments, synchronization of the image converter camera was accomplished by using an appropriate delay period in the camera control unit. The timing cycle was initiated when the gas mixture was ignited electrically. Thus, by selecting the proper delay time in the camera, it would gate the image tube at the time when the shock wave or flame would be in the desired observation position. The point-source lamp also received a trigger signal from the control unit so that the lamp would be pulsed during the time interval when the image tube was conducting. Both the pulsed light source and the image converter camera had to be operating at the precise time when the flame or shock wave was at the position in the detonation tube which was under investigation. The technique employed to synchronize the image converter tube and the point source lamp was to trigger the high-voltage gap tubes, which gated the image tube, by a voltage pulse derived from the point-source lamp as its storage capacitor discharged.

In some of the later experiments, a special phototube was utilized to start the timing cycle. When the flame passed the position of the phototube on the detonation tube wall, the output signal started the sequence of events. This method was most

successful when the phototube was situated at a position on the tube just upstream to that at which detonation occurs. The electrical output signal from the phototube was displayed on a dual-beam oscilloscope together with a signal which indicated the relative time of actuation of the image converter tube. The reason for changing to this arrangement is that the time delay derived from ignitor actuation was not too reliable; that is, there was a variation from one experiment to the next in the time required for the flame to progress from the ignitor to the position in the tube under investigation. A number of experiments were without results because of this variation. By using the phototube triggering technique, the reliability of getting a useful photograph was improved because the time interval between the position just prior to detonation and the position under study was fairly reproducible. Data from the pulses on the dual-beam oscilloscope were quite useful in predicting the time delay required to obtain an adequate photograph.

EXPERIMENTAL PROCEDURE

All experiments were conducted with a stoichiometric mixture of hydrogen and oxygen at an initial pressure of one atmosphere and at ambient initial temperatures. The detonation tube was evacuated and filled with the combustible mixture by the flow controls and equipment described in the previous section. After the experiment the tube was purged with dry air. The most critical part of the experimental procedure was that of selecting the correct delay times to obtain shadowgraphs of the flames and shock waves.

It was possible to move the shadowgraph system, illustrated in Fig. 3, to cover any part of the detonation tube from the ignitor to the impact end. For any position of the windows only certain portions of the test section in the detonation tube could be viewed. Full coverage was obtained by moving the windows and turning the side plates end-for-end. The ignitor could be inserted from either end of the tube. It was not feasible to use a single glass window to cover the entire length of the detonation tube.

The primary limitation of this shadowgraph system was its somewhat limited field of view. This restriction was caused by the six-inch diameter parabolic mirrors. Therefore, several experiments had to be performed at a particular nominal distance from the ignitor

in order to obtain adequate coverage of both the flame front and the shock wave. This procedure was complicated somewhat by the non-repeatable nature of the process of formation of a detonation wave even with identical initial conditions during the various experiments.

Initial experiments were conducted with the shadowgraph system positioned at the upstream end of the detonation tube where the ignitor was included in the field of view. A phototube, whose output was fed to a dual-beam oscilloscope, was positioned just downstream of the shadowgraph system to record the time of passage of the flame front at the particular position of the phototube. From these time intervals, approximate delay times were obtained for insertion into the delay unit which controlled the triggering time of the point-light source and that of the image converter camera. For the initial experiments the timing cycle was started when the ignitor button was depressed. Voltage pulses were sent to the oscilloscope and to the delay unit. As the delay times were increased, photographs of the flame and/or the shock front were obtained at increasing distances from the ignitor for a particular position of the shadowgraph system. Since the position of the fronts at a particular time were not exactly repeatable during successive experiments for the same initial conditions, some of the delay times were repeated for several experiments.

When the flame front passed out of the field of view (approximately 15 cm) of the shadowgraph system, the entire system was moved downstream, realigned, and refocused. These moves were made in increments of five to ten cm depending upon the amount of photographic coverage that had been obtained in the previous position. Approximately 45 cm of length of the detonation tube could be covered for a given position of the windows. After photographs of this area were obtained, the window positions were changed and the procedure was repeated. Measurements of the delay times were made during all experiments; the phototube was positioned either downstream or upstream of the shadowgraph system.

During some of the later experiments, when detonation or near-detonation conditions prevailed, the pulse from the phototube was used to trigger the delay unit and more repeatable results were obtained. This same procedure was tried when the transition mechanism was in its earlier stages, however, the results were no better than those obtained by using the ignitor-voltage pulse to trigger the delay unit.

Experiments were conducted with the ignitor at the one end of the tube to cover the region from the ignitor to a distance 44 cm downstream and from 80 to 110 cm from the ignitor. Then the ignitor was placed in the opposite end of the tube to obtain coverage from 40 to 167 cm from the reversed position of ignitor.

All shadowgraphs were recorded with film that had a 10-second development period; this technique permitted quick evaluation of the results and a decision could be made as to whether or not a specific delay time should be used in a repeat experiment. A camera was used also to record the oscilloscope images, the delay time, and the time of passage of the flame front past the phototube. Prints of the shadowgraphs with useful information were copied with regular negative-type film, and appropriate prints were made.

A black arrow-marker was placed on the window in the field of view of the shadowgraph system so that the relative position of specific events recorded on the photograph could be determined. The actual position was not given directly because of the magnification factor of the overall system. It was necessary to obtain the actual position of the flame and the shock wave relative to the ignitor; to obtain this distance, the relative distance was measured on the photographs. After converting to actual distances by use of the experimentally-determined magnification factor, the true position of the event under study could be located relative to the arrow-marker or the ignitor. By graphing the distance of the flame or shock fronts from the ignitor as a function of the delay time, the velocities of the fronts could be estimated up to a distance of approximately 80 cm from the ignitor (see Figs. 4 and 5). Beyond this distance, the results were not repeatable; therefore, no approximate velocities could be determined.

DISCUSSION OF RESULTS

In order to evaluate the data obtained during the investigation of the formation of detonations, the distances of the flame and shock fronts from the ignitor were plotted as a function of the delay times obtained from the oscilloscope trace; from these data average velocities of the fronts were estimated up to a distance of approximately 80 cm from the ignitor. Beyond this distance the nonrepeatability of the specific events made it practically impossible to obtain a reasonable estimate of the velocities. This region was

located just prior to that where detonation occurs; there the flame and shock fronts were greatly accelerated. Acceleration did not take place at the same position from one experiment to the next. Another factor that affected the results at this distance was the change in the window positions which altered the distance required for the formation of the detonation wave due to wave interactions caused by the slight gap, which was unavoidable, between the glass window and the side of the tube. Figure 4 shows the position of the leading edge of the flame front from the ignitor, and Fig. 5 depicts the distance from the ignitor to the leading shock wave taken from all of the photographs in which such a discontinuity was shown. The separation of the flame and shock fronts could be estimated from these data. Figures 6 and 7 are typical shadowgraphs of the discontinuities present during the formation of detonation; the photographs in Fig. 6 illustrate the reaction when the ignitor was at one end of the tube (end A) and those in Fig. 7 show the formation of detonation with the ignitor at the opposite end of the tube (end B).

From an analysis of the photographs of the reaction in the region next to the ignitor at end A, there appears to be a delay after closing the ignitor switch of the order of 200 to 300 microseconds (Fig. 4). The flame velocity just after ignition, is less than 100 m/sec and the flame front has a spherical shape (Fig. 6.1). Approximately 400 microseconds later (total delay of 600-700 microseconds), the flame front has contacted the top and bottom walls of the tube, and the leading edge of the flame front is 8 cm from the ignitor (Fig. 6.2). All time intervals and distances given are average values obtained during all of the experiments conducted at these conditions. The flame front now has a domed shape and some cellular structure is visible in the front (Figs. 6.3 and 6.4). However, the flame is laminar.

The flame front keeps the domed shape and the cellular structure until it is approximately 30 cm from the ignitor (Figs. 6.5 and 6.8). The first shock structure observed which precedes the flame front appears at a distance of approximately 33 cm from the ignitor with a total delay time of 1100 microseconds. At this time the flame front is 20 cm from the ignitor so that the separation between the shock and the flame fronts is 13 cm. These data were obtained from photographs, other than those shown, plus additional information derived from Figs. 4 and 5. Figure 6.6 is a typical photograph illustrating the series of shocks which is formed ahead of the flame front.

In the first series of pictures with the ignitor at end A of the tube, as the shock front approaches 38 cm distance from the ignitor, disturbances of a turbulent nature appear between the shock and flame front along the bottom of the detonation tube (Figs. 6.7, 6.8, 6.9 and 6.10). The disturbances have a rather peculiar structure that has a segmented appearance. When the flame front reaches 38 cm distance from the ignitor, the entire cross section of the unreacted gas, directly in front of the flame front, has a turbulent structure (Fig. 6.9). In fact, it is rather difficult to distinguish just where the flame front begins. There is a possibility that this region may consist of pockets of burning or exploding mixture, however, it is believed that the temperature is not sufficiently increased by shock-wave compression that auto-ignition could occur. The approximate velocity of the shock front in this region is 690 m/sec and the velocity of the flame is over 500 m/sec. The shock strength would have to be appreciably higher in order to compress the gas sufficiently, thereby raising its temperature, to ignite the combustible mixture.

The position of the windows in the first series of photographs was such that the viewing area ended 44 cm from the ignitor, and the glass window met the metal side of the tube at 46.4 cm. In some of the photographs obtained in this region, a reflected shock appears to be traveling in a direction which is opposite to that of the flame and shock fronts (Figs. 6.10 and 6.11). These shocks probably result from the slight gap that was present between the glass window and the side wall of the tube. The reflected shocks, in all probability, enhanced the formation of a detonation wave in the mixture; it has been shown (Ref. 47) that practically any type of turbulence-producing mechanism reduces the induction distance. Another explanation of the observed discontinuities, especially those in Fig. 6.10, is that they may be a secondary system of shocks following the leading shock front which does not appear in the photographs.

The next series of photographs was obtained with the glass windows positioned so that the leading edge of the viewing area was located 78.5 cm from the ignitor and the trailing edge at 124.2 cm (Figs. 6.12 to 6.16). The ignitor was located at the same position in the detonation tube as in the previous series of experiments. The region covered in this arrangement is from 79 cm to approximately 106 cm from the ignitor where the flame front approaches the shock front; the combined fronts have a concave shape. This region appears to be where the detonation wave is established. At approximately 100 cm from the ignitor, the front is practically normal to the sides of the detonation tube with no discernible flame structure in back of the front.

The reaction, now in full detonation, is still rather unstable, as is evident from the transverse disturbances visible behind the front. These transverse pressure fluctuations appear to be of the same nature as those observed by other investigators (Refs. 24 and 39) in their study of the formation of detonations. The fluctuations appear to be generated as a result of the passage of the detonation front; they start at the top or bottom of the detonation tube and move toward the opposite wall. Probably there are similar fluctuations across the tube from side to side, but they cannot be observed because a disturbance in that direction would not show in the shadowgraph system used. It is evident from these studies that the induction distance of the hydrogen-oxygen mixture used (66.67% hydrogen at one atmosphere initial pressure) is of the order of 90-100 cm when the ignitor is situated at end A of the tube and the glass windows are positioned to cover the region from 79 to 106 cm distance from the ignitor. However, it was found that the induction distance varies according to which end of the tube the ignitor is placed and also where the windows are positioned. It is obvious from these results that the tube was not completely symmetrical and that there was interference from surface discontinuities.

From the previously mentioned results it was expected that the shock and flame fronts should be at about the same positions from the ignitor for the same delay time if the ignitor were changed to the opposite end. However, the results obtained were quite different. With the ignitor positioned at end B of the tube and the windows placed to cover the region from 38.5 to 84.2 cm from the ignitor, a sequence of photographs, taken at a distance of approximately 43 cm, shows the leading shock wave to be about 20 cm in front of the flame front, corresponding to a time separation of 300 microseconds (Figs. 7.1 and 7.2). The flame front is still fairly laminar and there are no noticeable disturbances between the shock and flame fronts, which is in contrast to the results obtained with the ignitor in the opposite end at the same approximate position.

The velocity of the shock wave, rather constant in this region, is approximately 690 m/sec until it is 80 cm from the ignitor. The shock wave is shown farther downstream in Fig. 7.3. The propagation rate of the flame appears to be around 525 m/sec between 40 and 60 cm. At approximately 50 cm distance, the shape of the flame front begins to change and the portion along the top and bottom of the tube extends beyond the front in the center of the tube; also the flame front apparently changes from laminar to turbulent conditions (Figs. 7.4 and 7.5). Again, there are noticeable disturbances between the shock and flame front as there were at a distance of approximately 35 cm

when ignition was from the opposite end. The flame front apparently is giving off very strong pressure waves in this region (56-62 cm); they are readily visible on the shadowgraphs (Fig. 7.6 and 7.8). It is not very clear just where the flame front begins and where turbulence ends as the flame front itself becomes more wrinkled (Figs. 7.9, 7.11 and 7.13). In fact, approximately 62 cm from the ignitor it appears as if there are pockets of burning gases in the turbulent flow zone and there is no discernible flame front as such. That is, it appears that the flame front starts at the same region where turbulence is initiated.

One noticeable feature in this region is that the front extends farther forward on the bottom of the detonation tube than it does on the top in the majority of the photographs obtained. The structure as observed here is similar to the so-called tulip shape which has been observed by other investigators (Refs. 11 and 46) in their studies on the initiation of detonation. There is a moderate increase in the velocity of the overall flame front to about 610 m/sec, while the shock velocity remains at 690 m/sec at a distance of 80 cm from the ignitor. More shadowgraphs of the shock front in this region are shown in Figs. 7.7, 7.10, and 7.12. In Fig. 7.14 (marker distance 78 cm) the same type of segmented disturbances can be seen which was observed at approximately 38 cm (Figs. 6.10 and 6.11) with the ignitor at the opposite end. One significant feature in these experiments that differs from what was observed in other studies is the absence of a decrease in the velocity of the flame front soon after ignition which then is followed by an increase. According to the data obtained in this study, the propagation rate of the flame increases monotonically from ignition until a detonation wave is formed.

The shadowgraphs obtained at a marker distance of 78 cm from the ignitor show a reflected wave that propagates back toward the ignitor through the unreacted gas between the shock and flame fronts and which apparently is of sufficient strength to cause the gas to react (Fig. 7.15). The reflected shock is probably created when the leading shock wave passes the point on the tube at which the glass window and side wall meet. When the rearward-propagating shock wave and the forward-moving turbulent flame front meet, a small explosion apparently formed as indicated by the intense luminosity at that point (Fig. 7.16). This phenomenon, in all probability, created a detonation wave much sooner than if the tube wall had been completely smooth over the entire surface, which is the main reason why the data were not repeatable when the windows were changed from one position to another.

To obtain the next series of photographs, the window positions were changed to a location where the viewing area was between 79.5 to 125.2 cm from the ignitor. The first sequence of pictures taken in this region at a marker distance of 84 cm shows a type of reaction which is entirely different from that observed in the previous photographs. A reaction appears to be occurring wherein the flame front catches up to the leading shock wave. The flame front in Fig. 7.17 has a much different structure than that shown in the previous shadowgraphs. In this particular region the flame front apparently has accelerated greatly and has a streaked appearance as if not all of the mixture is being burned uniformly. After this type of structure was observed, a reaction occurs which has the form of an expanding pressure cell that forms immediately in front of the flame front and sends pressure waves into the unreacted and burned mixture (Figs. 7.18 to 7.26). These pressure cells apparently are created by explosions of the mixture in front of the moving flame front. An accurate determination of the pressures, temperatures, and velocities developed during this rapid reaction is rather difficult because of the limited data obtained. Schlieren strip film photographs in this region would help in determining the pertinent properties of the mixture between the shock and flame fronts.

These photographs do show that autoignition does not occur immediately behind the shock wave. If autoignition is to develop in the unreacted mixture between the shock and flame front, it is most likely to occur near the flame front where the temperature is highest. Strip-film photography studies by other investigators show that the leading shock wave during the build-up process is relatively weak; therefore, the shock is not of sufficient strength to increase the temperature of the gas to the autoignition level. According to Ref. 39, the Mach number of the shock wave just prior to detonation is 2.1 for a stoichiometric mixture of hydrogen and oxygen at one atmosphere initial pressure. The Mach number of the steady detonation wave is 5.3. For a specific heat ratio of 1.4, the temperature increases across a normal shock by a factor of 1.77 when the Mach number is 2.1. If the initial temperature were 25°C (ambient temperature), the increase would not be anywhere near the autoignition temperature for a mixture of hydrogen and oxygen.

Based on these results and other considerations, a more plausible explanation of the sequence of events is this. As the shock strength rises, the unreacted gas between the flame front and the shock is heated to a higher temperature by adiabatic compression. From various experimental studies, it is known that the burning velocity of a flame increases when the temperature of

the unreacted fuel-oxidizer mixture increases. The higher pressure also tends to increase the burning velocity of high-energy, fuel-oxidizer mixtures. These studies have not been conducted at very high temperatures of the unburned gas mixtures because of experimental difficulties. However, if the assumption is made, which appears reasonable, that the burning velocity increases as the temperature of the unreacted mixture increases to the value attained behind the shock wave, then the flame could travel forward much faster into the unreacted mixture and coalesce with the shock. This speed would be appreciably higher than that associated with values of normal burning velocities at normal ambient conditions. Although the rate of increase of the flame speed would be very fast, the reaction would not be a true explosion because of the temperature gradient which exists between the flame front and the shock wave.

Another factor, which may be significant, is that the velocity of the particles between the shock and flame front is supersonic with respect to the walls of the tube when the leading shock wave has a Mach number of 2.1. The turbulence level in the unreacted gas also would be a contributing factor to the explosion-like reaction. The boundary layer between the shock and flame front probably is turbulent and the "explosions" seem to originate near the walls of the tube. It is not clear at this time with the information available what, if any, connection there is between a turbulent boundary layer and the reaction as observed. It is practically impossible to estimate the velocities of the shock or flame fronts in this region because of the non-repeatability of the location of the reaction from one experiment to the next. This lack of information limits the discussion to what was obtained on the photographs with little reference to pressures, temperatures, etc.

After the flame fronts and the leading shock have merged, there appear to be several shocks formed prior to the actual formation of the detonation wave (Figs. 7.27, 7.28, 7.29, and 7.35). When the reaction appears to be in full detonation, the transverse pressure waves emanating from the front are visible again (Figs. 7.30 to 7.33) as was the case in the previous photographs with the ignitor on the opposite end. When the window positions were changed so that the area of coverage was from 120 cm to the impact end of the detonation tube, the reaction again was not in full detonation at a distance of 124 cm (Fig. 7.34) showing that the location of the windows had an influence on the formation of the detonation.

From Fig. 7.37 it is apparent that a detonation wave had not yet formed at a distance of 134.5 cm from the ignitor for that particular experiment. Although the majority of the photographs obtained in this region showed a detonation wave, the non-repeatable nature of certain events at specific distances from the ignitor is exemplified by this photograph. The shock structure which can be seen in back of the flame front could be a reflected shock propagating backward through the burning mixture which was formed when the leading shock wave passed the edge of the glass window located at 117.6 cm from the ignitor.

In Fig. 7.38 a detonation wave appears to be located at 138 cm, however, there also is a shock wave approximately 7.5 cm in front of the detonation wave. A sequence of photographs taken in this region, some of which are shown in Figs. 7.36, 7.39, and 7.40, shows that the distance between the detonation and shock waves decreases as they propagate down the tube. Apparently a detonation wave formed in the hot mixture behind the leading shock and the photographs show the shock wave being overtaken by the detonation wave. The velocity of the detonation wave would be much greater than that of the shock wave. The detonation wave probably was formed in the hot mixture because of the reflection of the leading shock wave at the edge of the glass window. The several shock fronts shown in Figs. 7.41 to 7.44 apparently were formed when the detonation wave merged with the leading shock wave.

The transverse pressure fluctuations back of the fully-developed detonation wave again are visible in Figs. 7.45 and 7.46. In Fig. 7.47 the detonation wave is shown just prior to impact at the end of the tube and in Fig. 7.48 the reflected wave can be observed.

CONCLUSIONS

An evaluation of the photographs indicates that upon ignition the burning process is laminar and that the propagation rate is relatively slow compared to detonation conditions. Thus, at a certain distance from the ignitor, the pressure waves emanating from the flame front coalesce into a shock wave which travels at a fairly constant rate (in this case 690 m/sec) until it is approximately 20 cm from the point at which a detonation wave is

formed. The flame front retains a domed shape after ignition until it is 40 to 60 cm from the ignitor; the distance is somewhat dependent on the tube configuration (position of the glass windows and associated surfaces).

The flame velocity up to this point increases constantly, but it is still somewhat slower than that of the shock wave; the separation between the shock and flame front is approximately 20 cm. As the flame front begins to lose its domed shape, some disturbances of a turbulent nature, ahead of the front, are recorded in some of the shadowgraphs. Then, the leading edge of the flame front travels along the walls and the whole front becomes turbulent; its apparent velocity increases rapidly. At approximately 80 to 100 cm from the ignitor, an explosion-like reaction takes place between the shock and flame front; this reaction is first noticeable near the flame front and the walls of the tube. This reaction apparently is created by the high-temperature and turbulence conditions of the boundary layer just in front of the flame front. These more-or-less point explosions generate pressure waves which are sent into both the unreacted and the burned gas. The waves propagating forward coalesce with the leading shock wave, which thereby is reinforced, and the waves traveling backward through the reacted gas form the so-called "retonation" wave.

When the pressure waves travel outward from the wall, they meet in the center of the tube, in some cases creating another "explosion" which again reinforces the leading shock wave. In this way the flame front overtakes the shock front, although not exactly by an increase in velocity of the flame front; instead it is a jump of the flame front to the shock front due to the localized explosion-like reactions which occur. It was definitely shown that there is no autoignition in back of the leading shock front. If autoignition occurred any place it was very close to the turbulent flame front. Another feature observed from the photographs was the transverse pressure fluctuations generated by the passage of the detonation wave. The exact reason for the presence of these has not been ascertained, but they appear to be the same type of pressure discontinuities which have been found during investigations of spinning and pulsating detonations.

As the reaction approaches the impact end of the detonation tube, a shock wave is observed in front of the detonation wave. Evidently a detonation wave was formed in the hot mixture which finally coalesced with the leading shock wave. The detonation

7

wave probably was formed because of a reflected shock which was created when the leading shock front passed the edge of the glass window upstream of the position at which this reaction was observed. It was evident from the results that changing the positions of the glass windows had changed the detonation induction distance. This non-symmetry did not greatly hinder the analysis because the main items of interest concerned the wave structures.

REFERENCES

1. Oppenheim, A. K.: A Contribution to the Theory of the Development and Stability of Detonation in Gases, *Journal of Applied Mechanics*, 19, No. 1, pp. 63-71, 1952.
2. Oppenheim, A. K.: Water-Channel Analog to High-Velocity Combustion, *Journal of Applied Mechanics*, pp. 115-121, March 1953.
3. Oppenheim, A. K.: Gasdynamic Analysis of the Development of Gaseous Detonation and its Hydraulic Analog, Fourth Symposium (International) on Combustion, The Williams & Wilkins Co., Baltimore, 1953.
4. Edse, R.: Calculations of Detonation Velocities in Gases, Wright Air Development Center Technical Report 54-416, ASTIA No. AD 94 173, March 1956.
5. Bollinger, L. E.: A Six Channel, Ten-Megacycle Chronograph for Supersonic Velocity Measurements, 11th Annual I.S.A. Conference, New York City, 17-21 Sept. 1956.
6. Bollinger, L. E., and Edse, R.: A Direct Measurement Technique of Determining Rocket Exhaust Velocities, Wright Air Development Center Technical Report 56-336, ASTIA No. AD 110 500, OTS #PB 121871, Nov. 1956.
7. Oppenheim, A. K.: On the Development of Gaseous Detonation, Memorandum, Institute of Engineering Research, University of California, Berkeley, Nov. 1956.
8. Bollinger, L. E., and Edse, R.: Measurement of Detonation Induction Distances in Hydrogen-Oxygen and Acetylene-Oxygen-Nitrogen Mixtures at Normal and Elevated Initial Pressures and Temperatures, Wright Air Development Center Technical Report 57-414, ASTIA No. AD 130 874, OTS #PB 131569, June 1957.
9. Bollinger, L. E., Measurement of Detonation Induction Distances in Combustible Gaseous Mixtures, *News in Engineering*, The Ohio State Univ., 29, No. 3, pp. 15-22, July 1957.
10. Bollinger, L. E.: One-Tenth Micro-Second, Multichannel Chronograph, *Australian Journ. Instr. Techn.*, 13, No. 3, pp. 97-104, Aug. 1957.

11. Martin, F. J.: Transition from Slow Burning to Detonation in Gaseous Explosions, General Electric Research Laboratory Report No. 58-RL-1936, April 1958.
12. Oppenheim, A. K., and Stern, R. A.: On the Development of Gaseous Detonation - I. Appraisal of the Problem, Technical Note DR1, University of California, Berkeley, June 1958.
13. Oppenheim, A. K., and Stern, R. A.: On the Development of Gaseous Detonation - II. Analysis of Wave Interaction Phenomena, Technical Note DR2, University of California, Berkeley, July 1958.
14. Hecht, G. J., Laderman, A. J., Stern, R. A., and Oppenheim, A. K.: On the Development of Gaseous Detonation - III. Ionization World Lines, Technical Note DR3, University of California, Berkeley, Jan. 1959.
15. Bollinger, L. E., and Edse, R.: Detonation Induction Distances in Combustible Gaseous Mixtures at Atmospheric and Elevated Initial Pressures. I Methane-Oxygen, II Carbon Monoxide - Oxygen, III Hydrogen-Oxygen, Wright Air Development Center Technical Report 58-591, ASTIA No. AD 208 325, OTS #PB 151873 March 1959.
16. Chu, S. T., and Edse, R.: Propagation of Sound Waves through Chemically Reacting Gas Mixtures, Proceedings of the Propellant Thermodynamics and Handling Conference, 20-21 July 1959, Special Report 12, Engineering Experiment Station, The Ohio State Univ., pp. 235-246, June 1960.
17. Edse, R.: Propagation of Shock Waves through Chemically Reacting Gas Mixtures, Proceedings of the Propellant Thermodynamics and Handling Conference, 20-21 July 1959, Special Report 12, Engineering Experiment Station, The Ohio State Univ., pp. 247-258, June 1960.
18. Bollinger, L. E., and Edse, R.: Effect of Initial Pressure and Temperature on the Detonation Induction Distances in Hydrogen-Oxygen and Acetylene-Oxygen-Nitrogen Mixtures, Proceedings of the Propellant Thermodynamics and Handling Conference, 20-21 July 1959, Special Report 12, Engineering Experiment Station, The Ohio State Univ., pp. 441-456, June 1960.

19. Bollinger, L. E., Fong, M. C., and Edse, R.: Detonation Induction Distances in Combustible Gaseous Mixtures at Atmospheric and Elevated Initial Pressures. IV Hydrogen-Nitric Oxide, V Hydrogen-Oxygen-Diluent, VI Theoretical Analysis, Wright Air Development Center Technical Report 58-591 (Part II), ASTIA No. AD 239 677, OTS #PB 161878, Aug. 1959.
20. Bollinger, L. E., Fong, M. C., and Edse, R.: Theoretical Analysis and Experimental Measurements of Detonation Induction Distances at Atmospheric and Elevated Initial Pressures, American Rocket Society Meeting, Washington, D. C., Paper No. 922-59, Nov. 1959.
21. Stern, R. A., and Oppenheim, A. K.: Fundamentals of the Polar Method in Gas Wave Dynamics, Technical Note DR5, University of California, Berkeley, Nov. 1959.
22. Stern, R. A., Laderman, A. J., and Oppenheim, A. K.: Statistical Study of Accelerating Flames - Analysis of Variance, Technical Note DR6, University of California, Berkeley, Nov. 1959.
23. Gross, R. A., and Oppenheim, A. K.: Recent Advances in Gaseous Detonation, ARS Journal, 29, No. 3, pp. 173-179, 1959.
24. Zeldovich, Ia. B., and Kompaneets, A. S.: Theory of Detonation, Academic Press Inc., London, 1960.
25. Oppenheim, A. K., and Stern, R. A.: Development and Structure of Plane Detonation Waves, Technical Note DR7, University of California, Berkeley, Feb. 1960.
26. Hecht, G. J., Laderman, A. J., Stern, R. A., and Oppenheim, A. K.: Determination of Flame Velocities in Gaseous Predetonation, The Review of Scientific Instruments, 31, No. 10, pp. 1107-1111, Oct. 1960.
27. Laderman, A. J., and Oppenheim, A. K.: Experimental Study of the Development of Detonation, Technical Note DR9, University of California, Berkeley, Nov. 1960.
28. Bollinger, L. E., Fong, M. C., Halagan, D. R., and Edse, R.: Experimental and Theoretical Investigation of the Fluid Dynamics of Rocket Combustion, Aeronautical Research Laboratories Technical Note 60-141, ASTIA No. AD 249 696, OTS #PB 154259, Nov. 1960.

29. Fishburne, E. S., and Edse, R.: Detonability of Ozone and Nitric Oxide, Vol. 2, ARS Progress in Astronautics and Rocketry, Liquid Rockets and Propellants, Academic Press, Nov. 1960.
30. Laderman, A. J., Hecht, G. J., Stern, R. A., and Oppenheim, A. K.: Flame Ionization During the Development of Detonation, Eighth Symposium (International) on Combustion, The Williams & Wilkins Co., Baltimore, 1960.
31. Oppenheim, A. K., Stern, R. A., and Urtiew, P. A.: On the Development of Detonation with Pre-Ignition, Combustion and Flame, 1960.
32. Baumann, W., Urtiew, P. A., and Oppenheim, A. K.: Photographic Observation of Accelerating Flames, AFOSR TN-60-932, University of California, Berkeley, 1960.
33. Bollinger, L. E., and Edse, R.: Thermodynamic Calculations of Hydrogen-Oxygen Detonation Parameters for Various Initial Pressures, ARS Journal, 31, No. 2, pp. 251-256, Feb. 1961.
34. Bollinger, L. E., Fong, M. C., and Edse, R.: Experimental Measurements and Theoretical Analysis of Detonation Induction Distances, ARS Journal, 31, No. 5, pp. 588-595, May 1961.
35. Fong, M. C., Bollinger, L. E., and Edse, R.: Magnetohydrodynamic Effects on Exothermal Waves, I. Theoretical Problems on a Macroscopic Scale, II. Experimental Study with Hydrogen-Oxygen Detonation Waves, Aeronautical Research Laboratories Technical Report 69, ASTIA No. AD 269 280, Sept. 1961.
36. Bollinger, L. E., Laughrey, J. A., and Edse, R.: Experimental Detonation Velocities and Induction Distances in Hydrogen - Nitrous Oxide Mixtures, ARS Journal, 32, No. 1, pp. 81-82, Jan. 1962.
37. Bollinger, L. E., Laughrey, J. A., and Edse, R.: Effect of Ignition Method on Detonation Induction Distances in Hydrogen-Oxygen Mixtures, ARS Journal, 32, No. 3, pp. 428-430, March 1962.
38. Bollinger, L. E., Nicholson, J. R., Krisjansons, J. O., Fishburne, E. S., and Edse, R.: Fluid Dynamics of Rocket Combustion, Aeronautical Research Laboratories Technical Report 62-323, ASTIA No. AD 277 901, April 1962.

39. Oppenheim, A. K., Laderman, A. J., and Urtiew, P. A.: The Onset of Retonation, Combustion and Flame, 6, No. 3, Butterworths Publications, London, Sept. 1962.
40. Laughrey, J. A., Bollinger, L. E., and Edse, R.: Detonability of Nitrous Oxide at Elevated Initial Pressures and Temperatures, Aeronautical Research Laboratories Technical Report 62-432, Sept. 1962.
41. Bollinger, L. E., and Edse, R.: Thermodynamic Calculations of Carbon Monoxide - Air Detonation Parameters for Initial Pressures from 1 to 100 Atmospheres, NASA Technical Note D-1667, Dec. 1962.
42. Krisjansons, J. O., Bollinger, L. E., and Edse, R.: Explosion Limit Studies of Nitrous Oxide and Nitrous Oxide - Nitrogen-Air Mixtures to 200 Atm. and 1800°R, Aeronautical Research Laboratories Technical Report 62-431, Sept. 1962.
43. Fishburne, E. S., and Edse, R.: Chemical Kinetics of Nitrous Oxide Decomposition at Elevated Pressures and Temperatures, Aeronautical Research Laboratories Technical Report 62-430, Sept. 1962.
44. Laderman, A. J., Urtiew, P. A., and Oppenheim, A. K.: Measurement of Pressure Field Generated at the Initiation of Explosion, Symposium on Measurement in Unsteady Flow by the American Society of Mechanical Engineers, 1962.
45. Laderman, A. J., and Oppenheim, A. K.: Initial Flame Acceleration in an Explosive Gas, Proceedings of the Royal Society, A, 268, pp. 153-180, 1962.
46. Pyatnitskii, L. N.: Flame Acceleration Mechanism in the Transition of Normal Combustion to Detonation, Soviet Physics-Doklady, 7, No. 6, pp. 495-498, Dec. 1962.
47. Bollinger, L. E., Fong, M. C., Laughrey, J. A., and Edse, R.: Experimental and Theoretical Studies on the Formation of Detonation Waves in Variable Geometry Tubes, NASA Technical Note D-1983, June 1963.
48. Bollinger, L. E.: Formation of Detonation Waves in Hydrogen-Oxygen Mixtures from 0.2 to 2 Atmospheres Initial Pressure in a 54-Meter Long Tube, NASA Technical Note (in press).

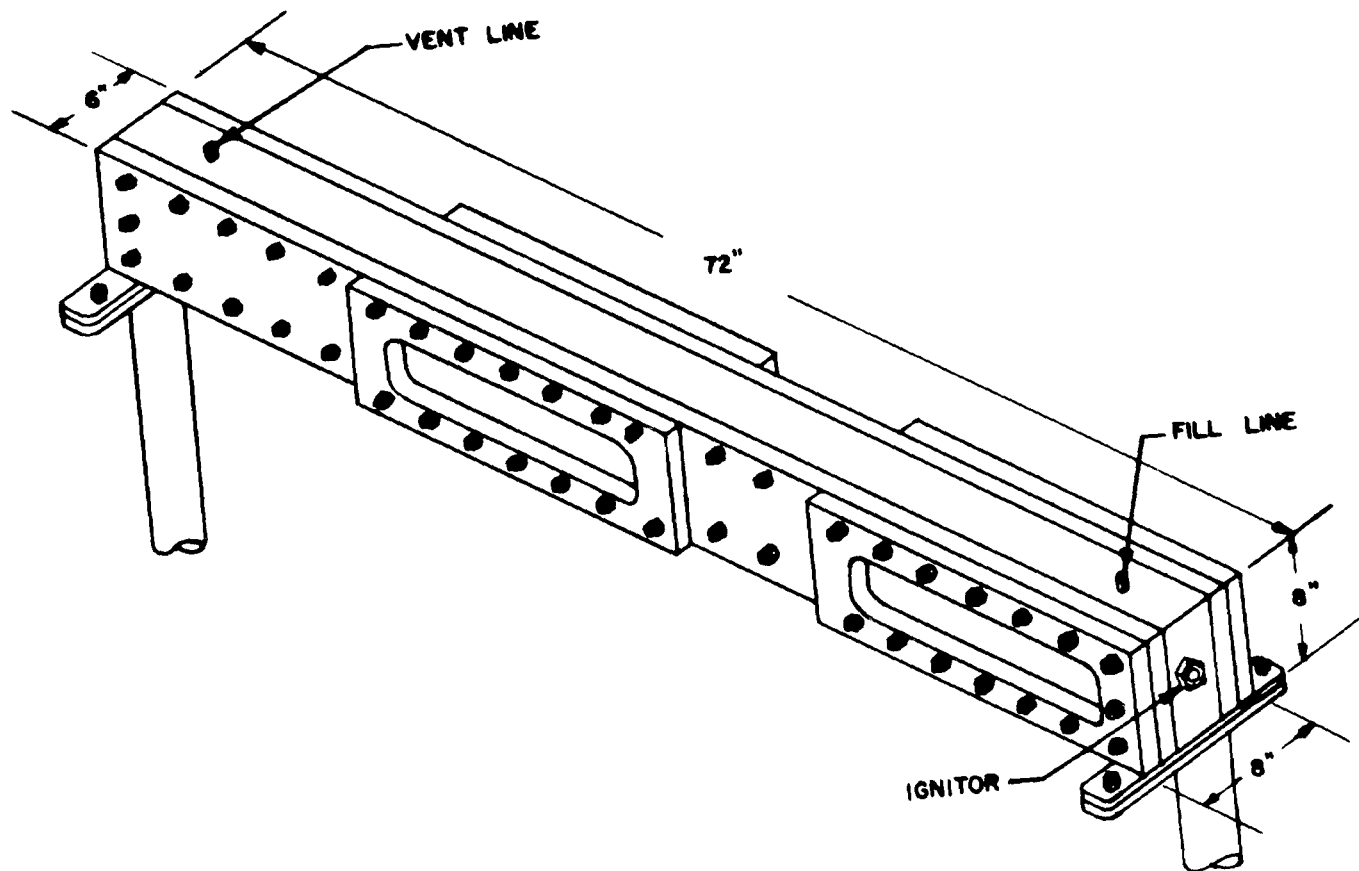


FIG. 1 PICTORIAL VIEW OF DETONATION TUBE

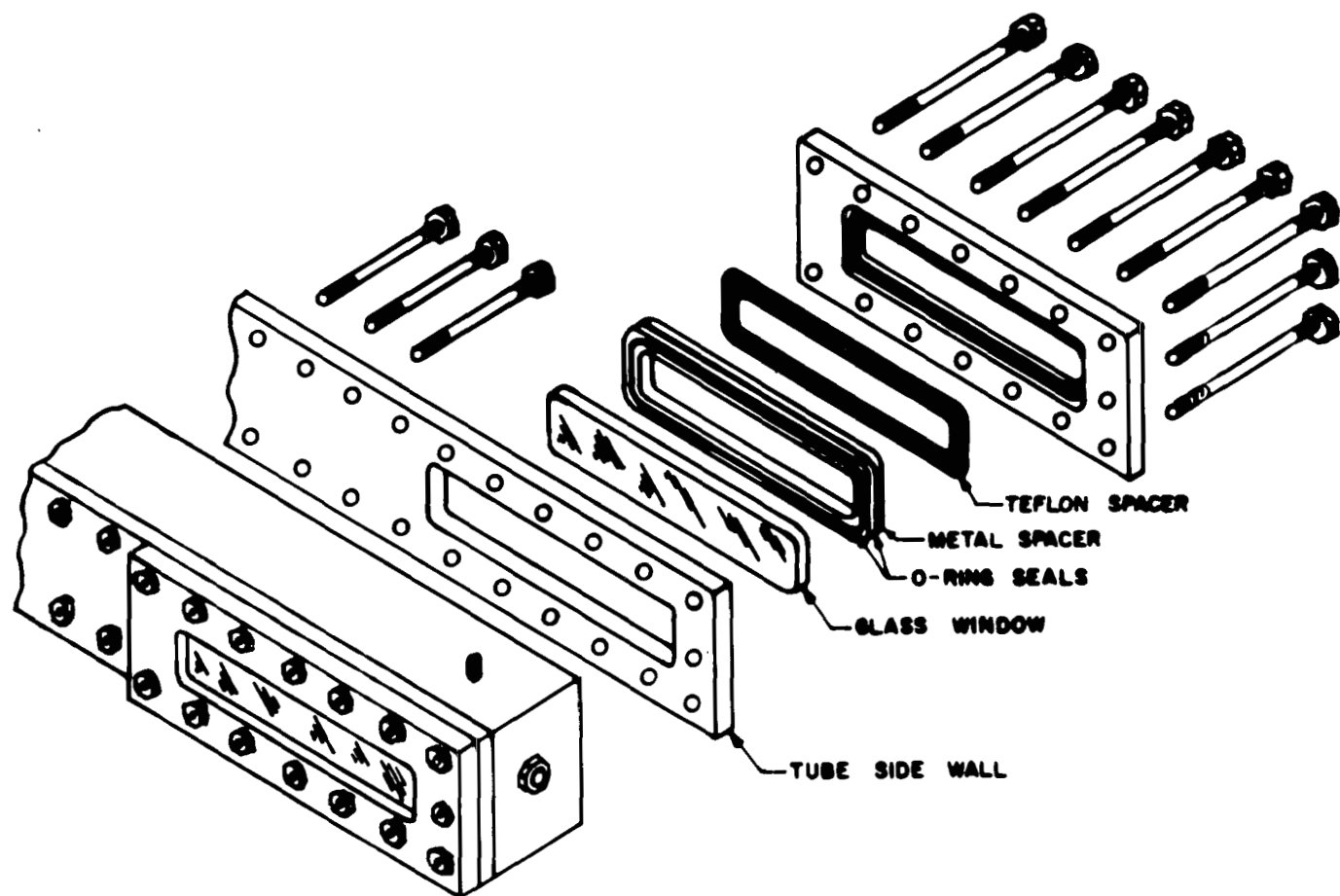


FIG. 2 EXPLODED VIEW OF DETONATION-TUBE WINDOW

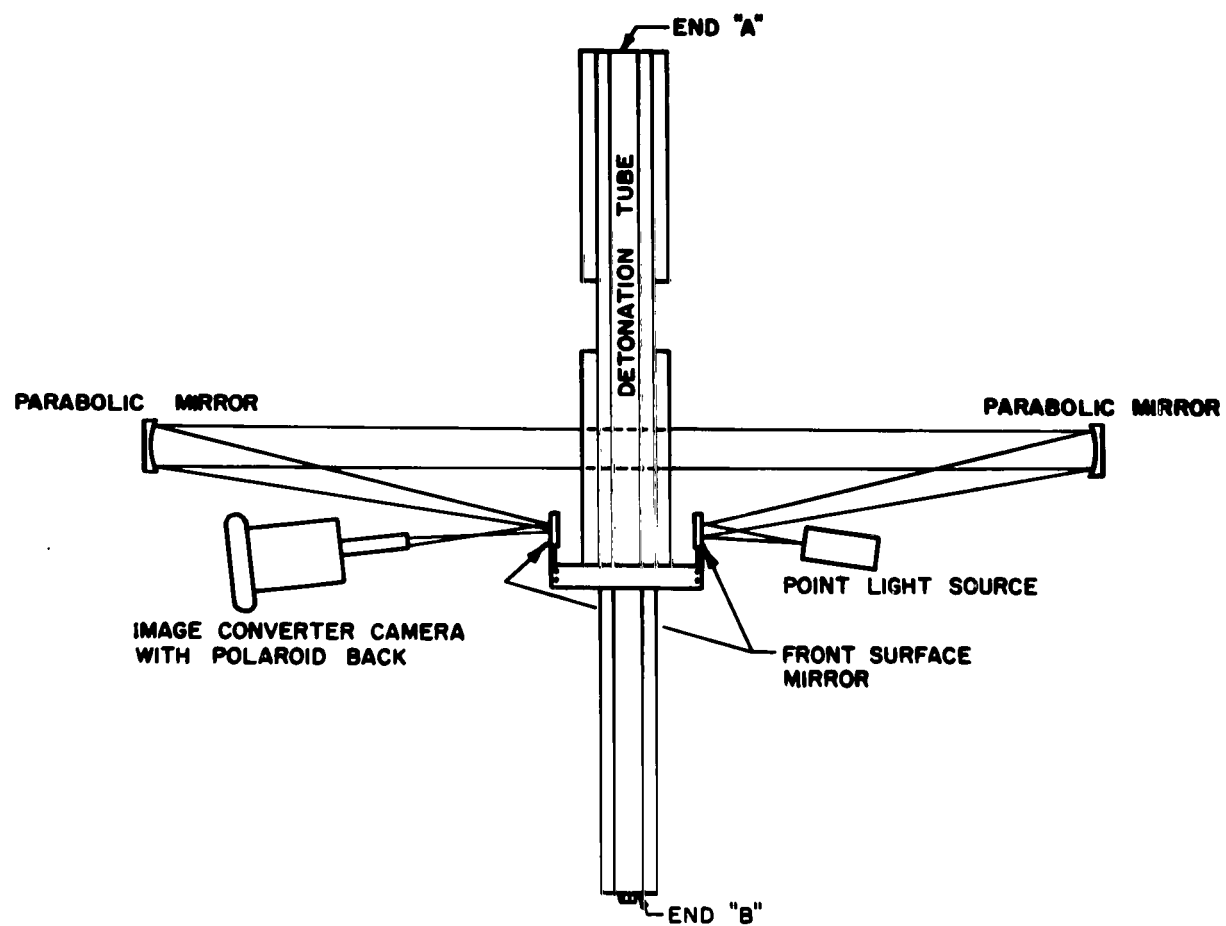


FIG. 3 DIAGRAM OF SHADOWGRAPH SYSTEM

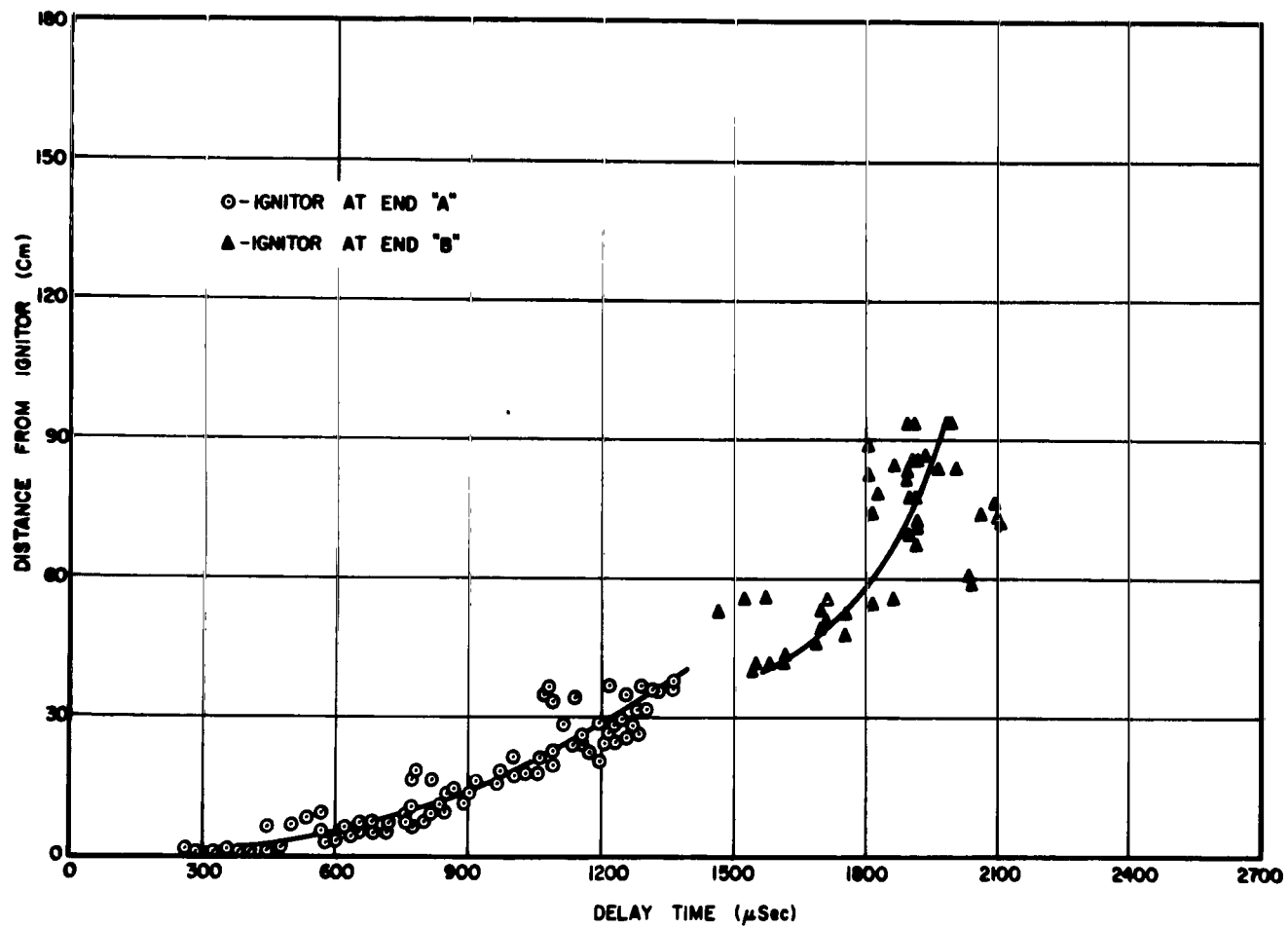


FIG. 4 DISTANCE OF FLAME FRONT FROM IGNITOR

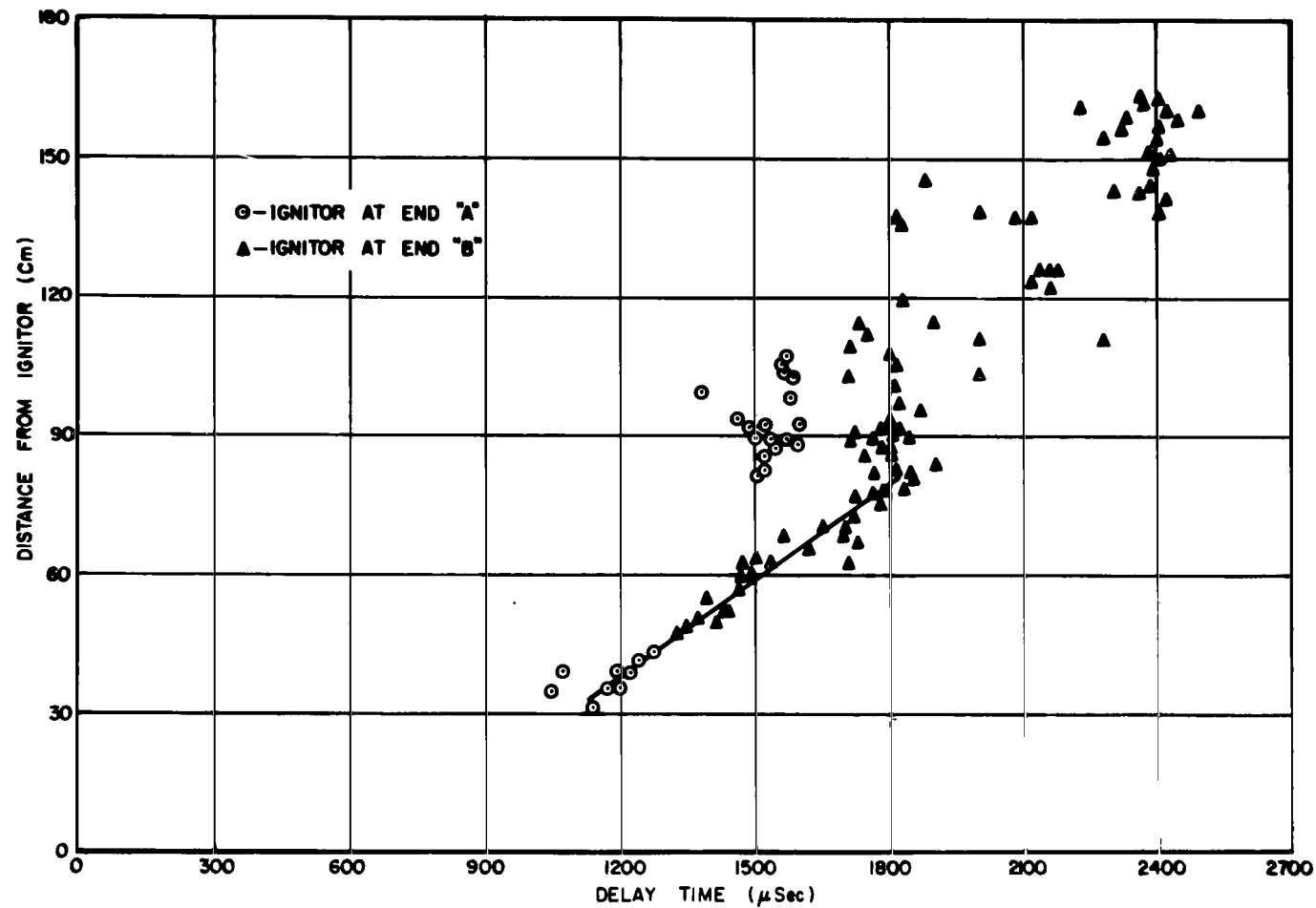
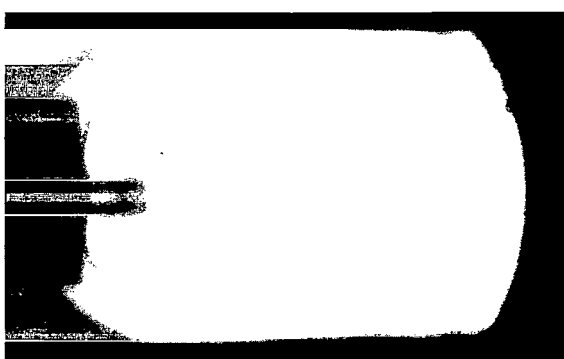


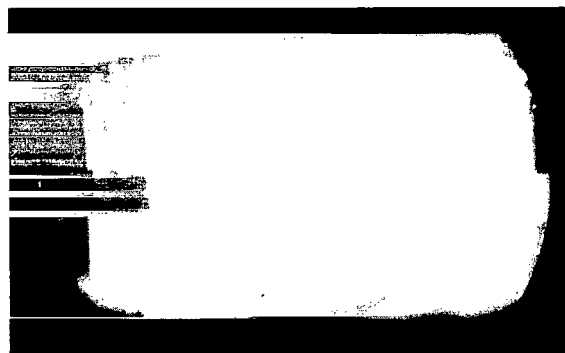
FIG. 5 DISTANCE OF SHOCK OR DETONATION FRONT FROM IGNITOR



(6.1)

DISTANCE FROM IGNITOR (Cm)

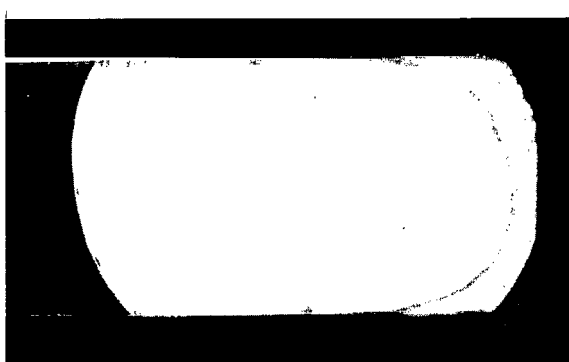
MARKER	0
FLAME FRONT	2
SHOCK FRONT	NOT IN VIEW



(6.2)

DISTANCE FROM IGNITOR (Cm)

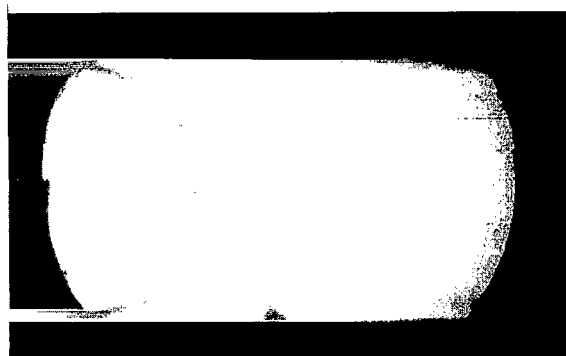
MARKER	0
FLAME FRONT	8.3
SHOCK FRONT	NOT IN VIEW



(6.3)

DISTANCE FROM IGNITOR (Cm)

MARKER	12
FLAME FRONT	17.2
SHOCK FRONT	NOT IN VIEW

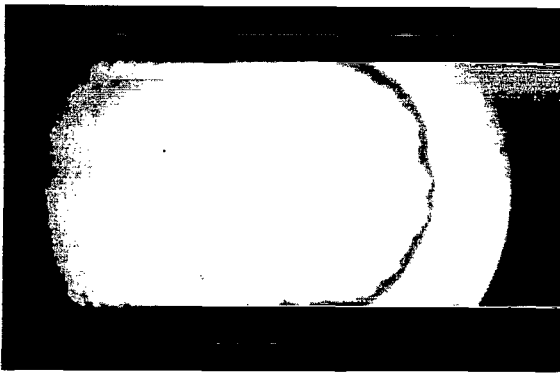


(6.4)

DISTANCE FROM IGNITOR (Cm)

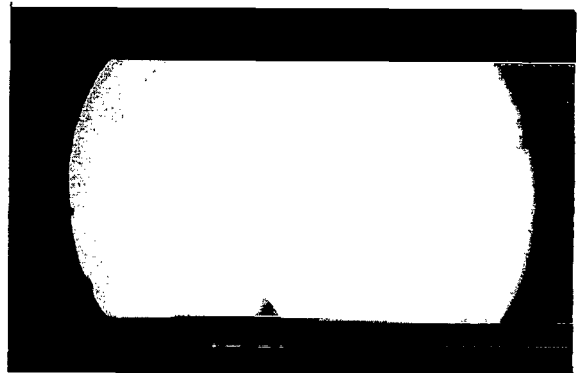
MARKER	20
FLAME FRONT	17.7
SHOCK FRONT	NOT IN VIEW

FIG. 6 SHADOWGRAPHS OF THE FORMATION OF THE DETONATION WAVE; IGNITION AT END A.



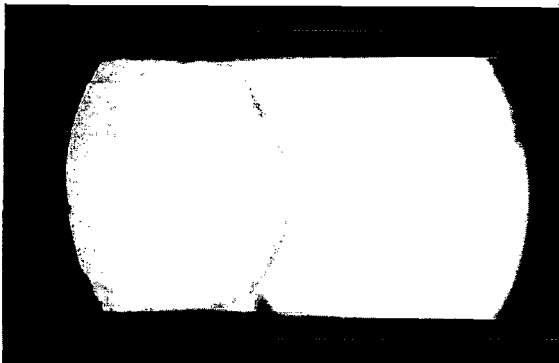
(6.5)

DISTANCE FROM IGNITOR (Cm)	
MARKER	25
FLAME FRONT	29
SHOCK FRONT	NOT IN VIEW



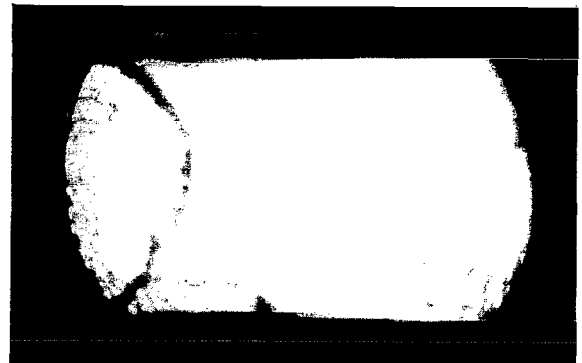
(6.6)

DISTANCE FROM IGNITOR (Cm)	
MARKER	33
FLAME FRONT	NOT IN VIEW
SHOCK FRONT	39.5



(6.7)

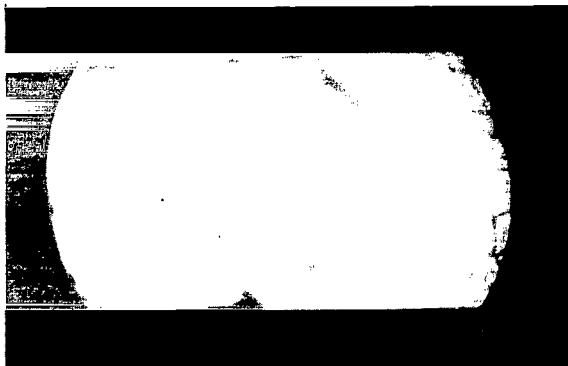
DISTANCE FROM IGNITOR (Cm)	
MARKER	33
FLAME FRONT	31
SHOCK FRONT	NOT IN VIEW



(6.8)

DISTANCE FROM IGNITOR (Cm)	
MARKER	33
FLAME FRONT	33.7
SHOCK FRONT	NOT IN VIEW

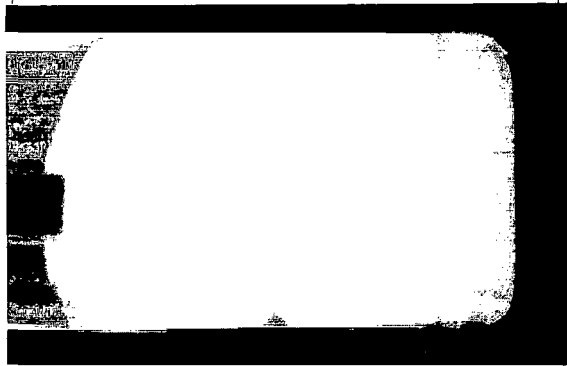
FIG. 6 (CONT'D) SHADOWGRAPHS OF THE FORMATION OF THE DETONATION WAVE; IGNITION AT END A.



(6.9)

DISTANCE FROM IGNITOR (Cm)

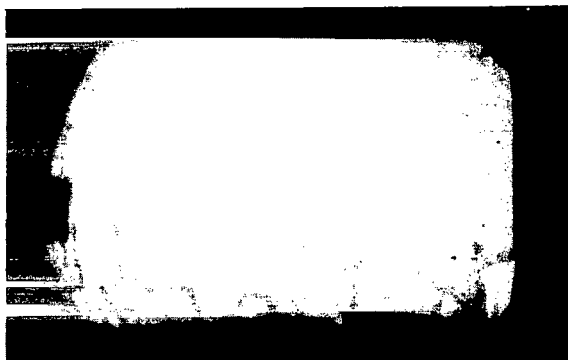
MARKER	33
FLAME FRONT	36.4
SHOCK FRONT	NOT IN VIEW



(6.10)

DISTANCE FROM IGNITOR (Cm)

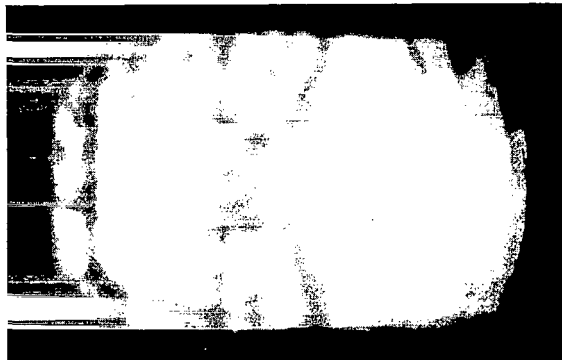
MARKER	38
FLAME FRONT	NOT IN VIEW
SHOCK FRONT	42



(6.11)

DISTANCE FROM IGNITOR (Cm)

MARKER	38
FLAME FRONT	NOT IN VIEW
SHOCK FRONT	45.2



(6.12)

DISTANCE FROM IGNITOR (Cm)

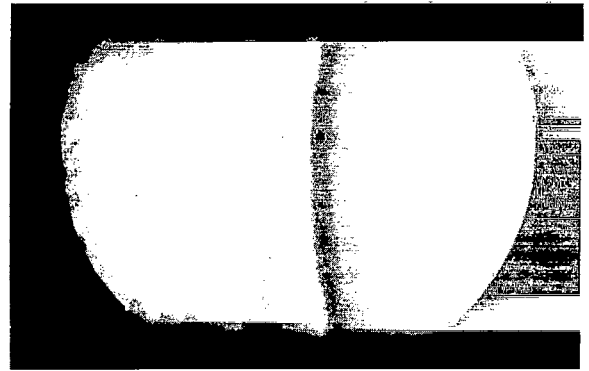
MARKER	85
FLAME FRONT	85
SHOCK FRONT	85

FIG. 6 (CONT'D) SHADOWGRAPHS OF THE FORMATION OF THE DETONATION WAVE; IGNITION AT END A.



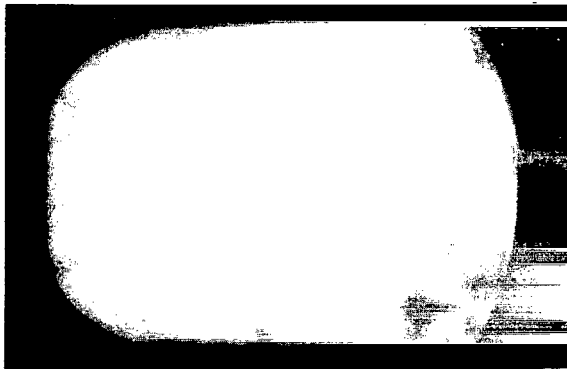
(6.13)

DISTANCE FROM IGNITOR (Cm)	
MARKER	85
FLAME FRONT	89
SHOCK FRONT	89



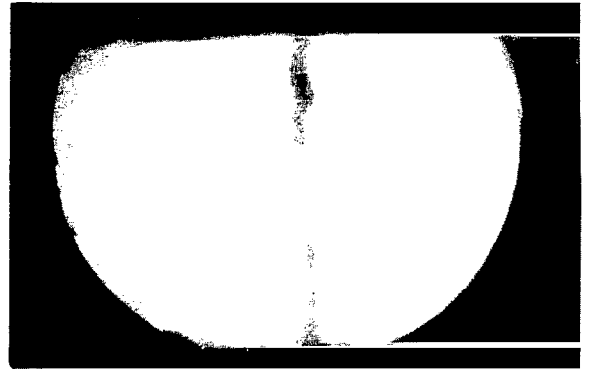
(6.14)

DISTANCE FROM IGNITOR (Cm)	
MARKER	90
FLAME FRONT	91.9
SHOCK FRONT	91.9



(6.15)

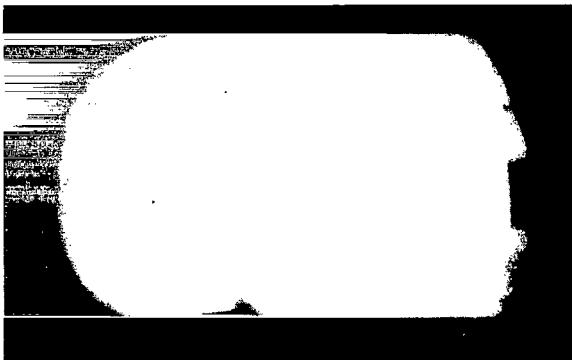
DISTANCE FROM IGNITOR (Cm)	
MARKER	90
FLAME FRONT	NOT IN VIEW
SHOCK FRONT	NOT IN VIEW



(6.16)

DISTANCE FROM IGNITOR (Cm)	
MARKER	100
FLAME FRONT	NOT IN VIEW
SHOCK FRONT	102.6

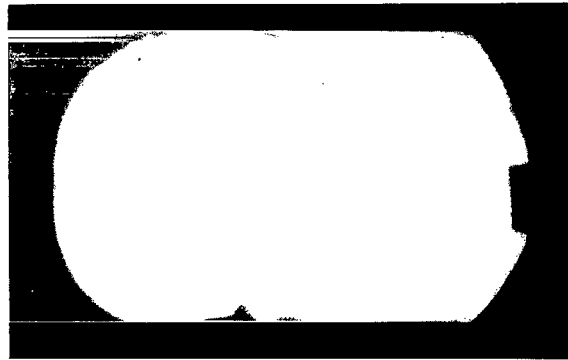
FIG. 6 (CONT'D) SHADOWGRAPHS OF THE FORMATION OF THE DETONATION WAVE; IGNITION AT END A.



(7.1)

DISTANCE FROM IGNITOR (Cm)

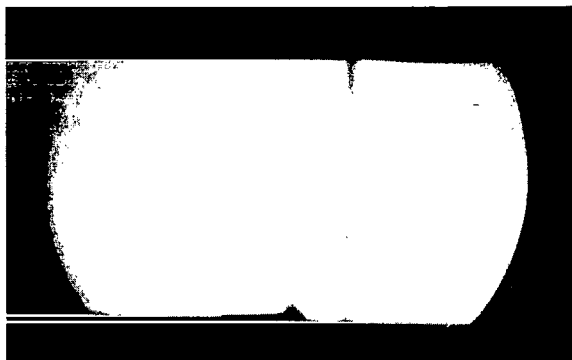
MARKER	43
FLAME FRONT	NOT IN VIEW
SHOCK FRONT	43.6



(7.2)

DISTANCE FROM IGNITOR (Cm)

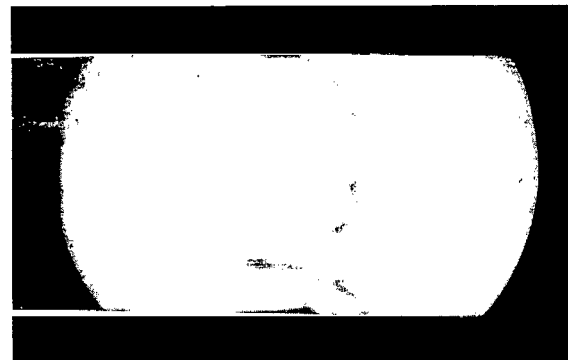
MARKER	43
FLAME FRONT	46.3
SHOCK FRONT	NOT IN VIEW



(7.3)

DISTANCE FROM IGNITOR (Cm)

MARKER	51
FLAME FRONT	NOT IN VIEW
SHOCK FRONT	52.7

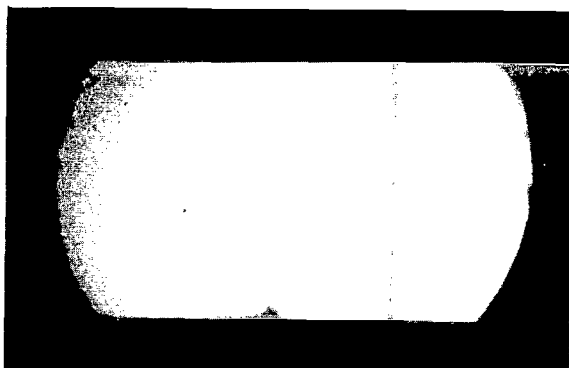


(7.4)

DISTANCE FROM IGNITOR (Cm)

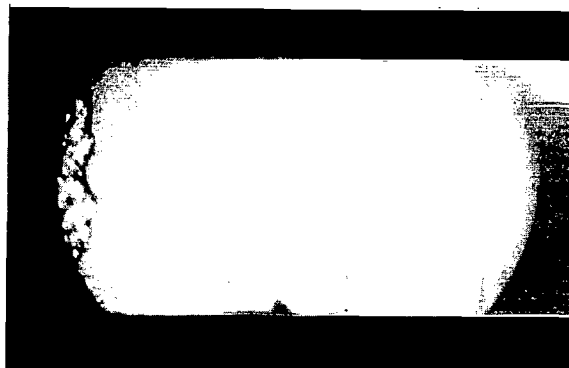
MARKER	51
FLAME FRONT	52.5
SHOCK FRONT	NOT IN VIEW

FIG. 7 SHADOWGRAPHS OF THE FORMATION OF THE DETONATION WAVE; IGNITION AT END B.



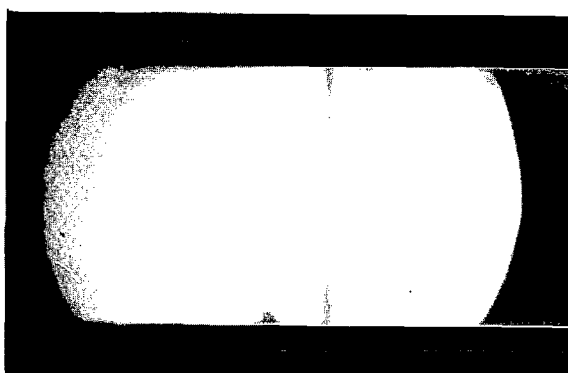
(7.5)

DISTANCE FROM IGNITOR (Cm)	
MARKER	56
FLAME FRONT	NOT IN VIEW
SHOCK FRONT	59.6



(7.6)

DISTANCE FROM IGNITOR (Cm)	
MARKER	56
FLAME FRONT	50.6
SHOCK FRONT	62.1



(7.7)

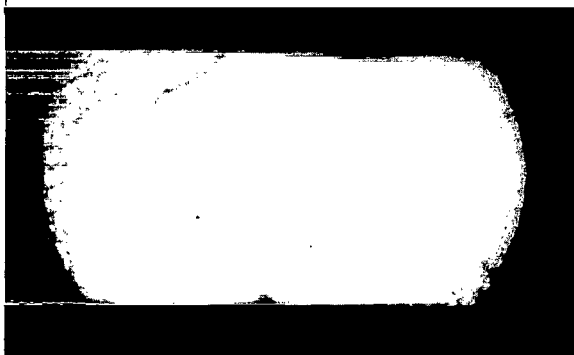
DISTANCE FROM IGNITOR (Cm)	
MARKER	62
FLAME FRONT	NOT IN VIEW
SHOCK FRONT	63.8



(7.8)

DISTANCE FROM IGNITOR (Cm)	
MARKER	62
FLAME FRONT	63.3
SHOCK FRONT	NOT IN VIEW

FIG. 7 (CONT'D) SHADOWGRAPHS OF THE FORMATION OF THE
DETONATION WAVE; IGNITION AT END B.



(7.9)

DISTANCE FROM IGNITOR (cm)	
MARKER	62
FLAME FRONT	NOT IN VIEW
SHOCK FRONT	NOT IN VIEW



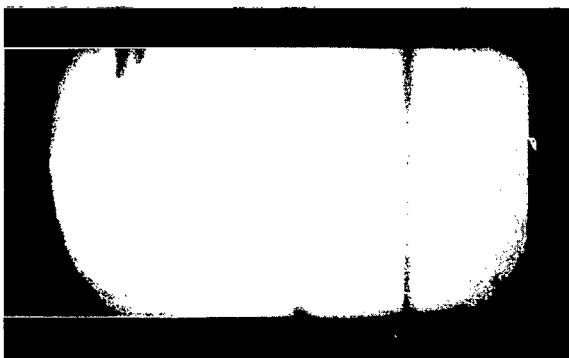
(7.10)

DISTANCE FROM IGNITOR (cm)	
MARKER	70
FLAME FRONT	NOT IN VIEW
SHOCK FRONT	75.4



(7.11)

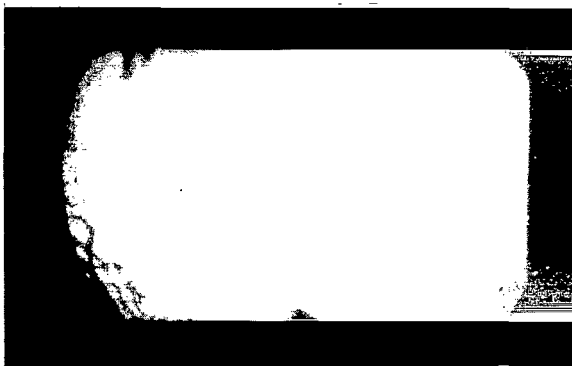
DISTANCE FROM IGNITOR (cm)	
MARKER	70
FLAME FRONT	73.4
SHOCK FRONT	NOT IN VIEW



(7.12)

DISTANCE FROM IGNITOR (cm)	
MARKER	78
FLAME FRONT	NOT IN VIEW
SHOCK FRONT	81.1

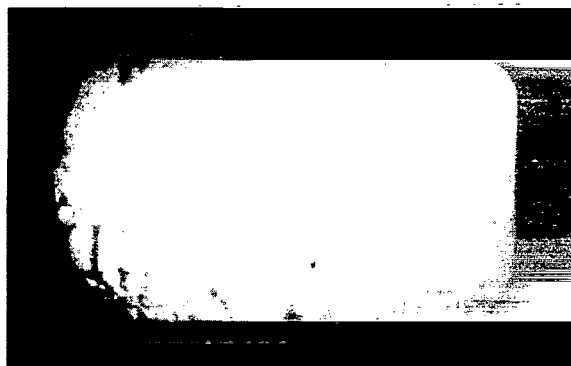
FIG. 7 (CONT'D) SHADOWGRAPHS OF THE FORMATION OF THE DETONATION WAVE; IGNITION AT END B.



(7.13)

DISTANCE FROM IGNITOR (Cm)

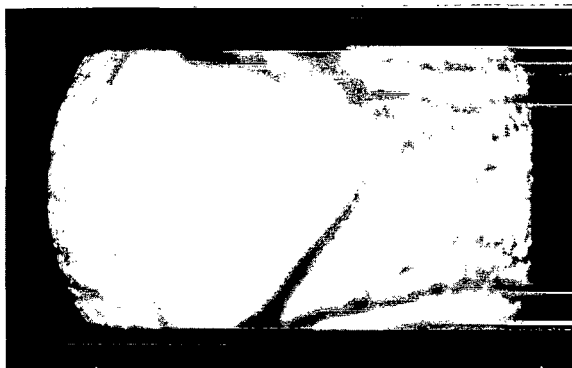
MARKER	78
FLAME FRONT	78
SHOCK FRONT	NOT IN VIEW



(7.14)

DISTANCE FROM IGNITOR (Cm)

MARKER	78
FLAME FRONT	NOT IN VIEW
SHOCK FRONT	NOT IN VIEW



(7.15)

DISTANCE FROM IGNITOR (Cm)

MARKER	78
FLAME FRONT	74
SHOCK FRONT	NOT IN VIEW

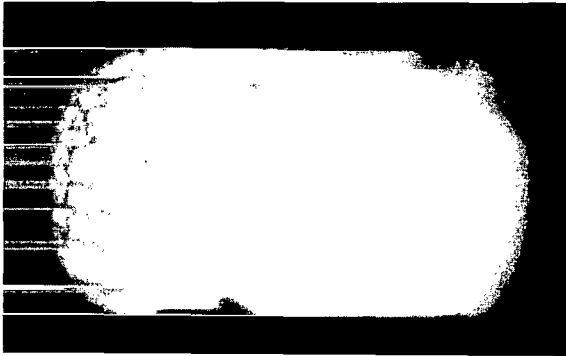


(7.16)

DISTANCE FROM IGNITOR (Cm)

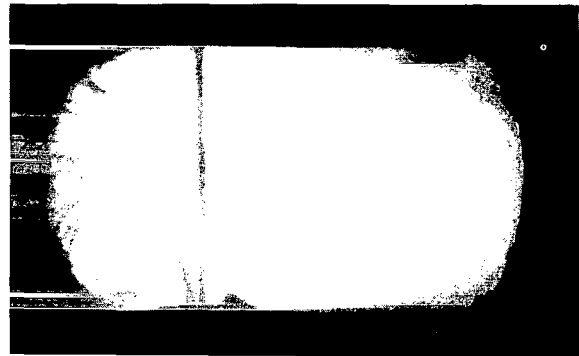
MARKER	78
FLAME FRONT	UNKNOWN
SHOCK FRONT	UNKNOWN

FIG. 7 (CONT'D) SHADOWGRAPHS OF THE FORMATION OF THE DETONATION WAVE; IGNITION AT END B.



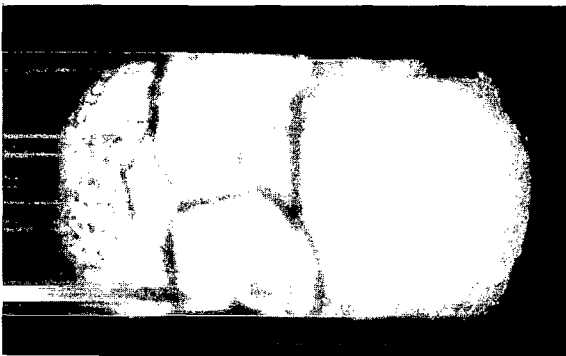
(7.17)

DISTANCE FROM IGNITOR (Cm)	
MARKER	84
FLAME FRONT	85.1
SHOCK FRONT	NOT IN VIEW



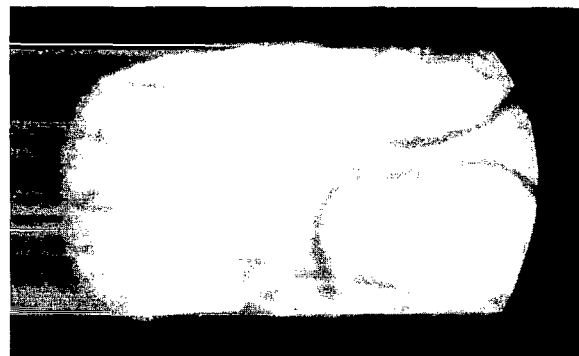
(7.18)

DISTANCE FROM IGNITOR (Cm)	
MARKER	84
FLAME FRONT	83
SHOCK FRONT	83.3



(7.19)

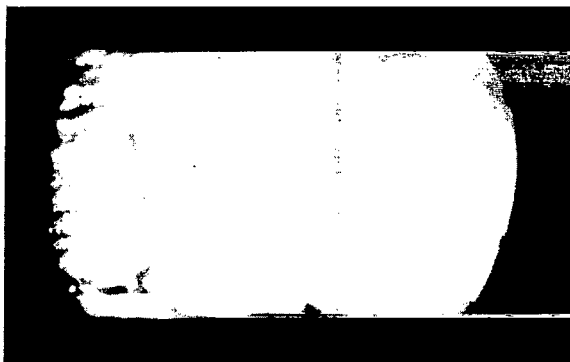
DISTANCE FROM IGNITOR (Cm)	
MARKER	84
FLAME FRONT	85.6
SHOCK FRONT	85.6



(7.20)

DISTANCE FROM IGNITOR (Cm)	
MARKER	84
FLAME FRONT	NOT IN VIEW
SHOCK FRONT	NOT IN VIEW

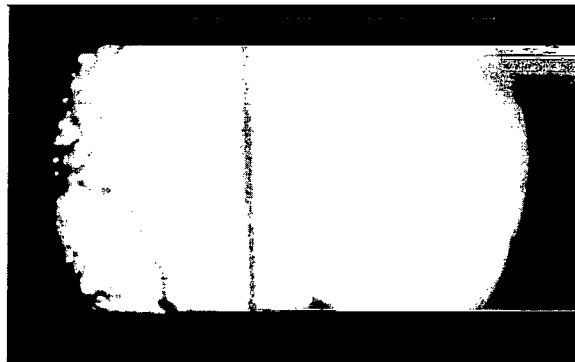
FIG. 7 (CONT'D) SHADOWGRAPHS OF THE FORMATION OF THE DETONATION WAVE; IGNITION AT END B.



(7.21)

DISTANCE FROM IGNITOR (Cm)

MARKER	92
FLAME FRONT	88.9
SHOCK FRONT	93.1



(7.22)

DISTANCE FROM IGNITOR (Cm)

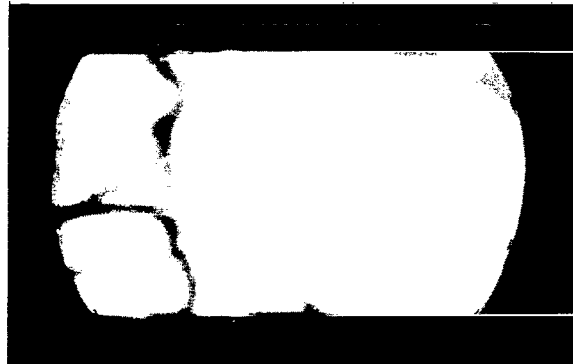
MARKER	92
FLAME FRONT	88
SHOCK FRONT	90.2



(7.23)

DISTANCE FROM IGNITOR (Cm)

MARKER	92
FLAME FRONT	90.2
SHOCK FRONT	90.2

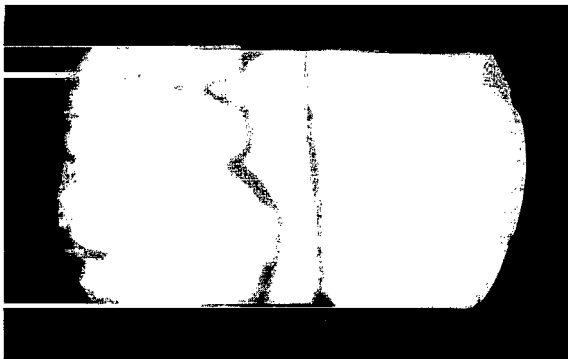


(7.24)

DISTANCE FROM IGNITOR (Cm)

MARKER	92
FLAME FRONT	89.8
SHOCK FRONT	89.8

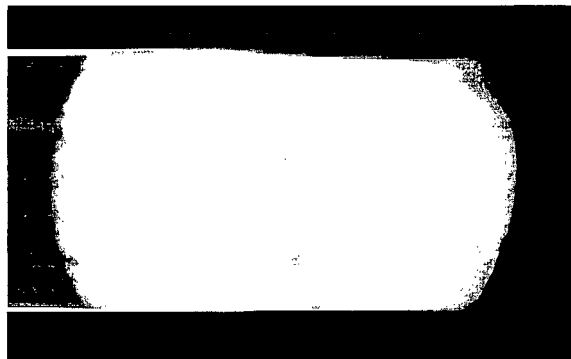
FIG. 7 (CONT'D) SHADOWGRAPHS OF THE FORMATION OF THE DETONATION WAVE; IGNITION AT END B.



(7.25)

DISTANCE FROM IGNITOR (Cm)

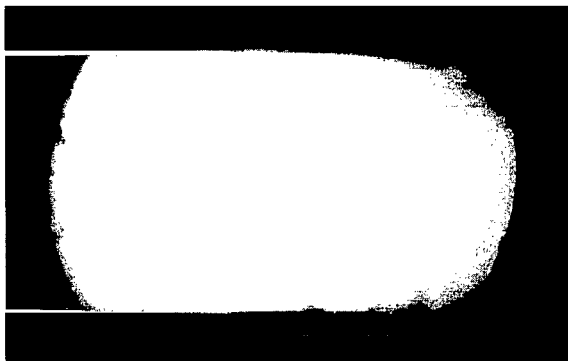
MARKER	92
FLAME FRONT	91.1
SHOCK FRONT	92



(7.26)

DISTANCE FROM IGNITOR (Cm)

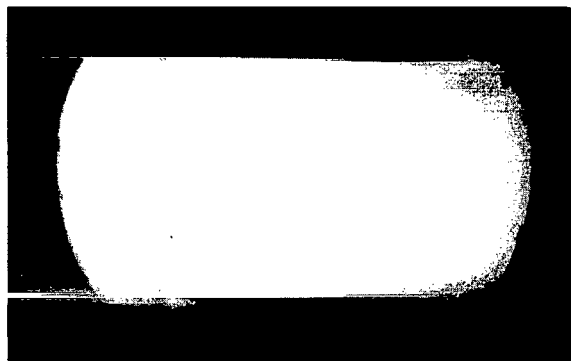
MARKER	92
FLAME FRONT	93.6
SHOCK FRONT	NOT IN VIEW



(7.27)

DISTANCE FROM IGNITOR (Cm)

MARKER	92
FLAME FRONT	NOT IN VIEW
SHOCK FRONT	95.1

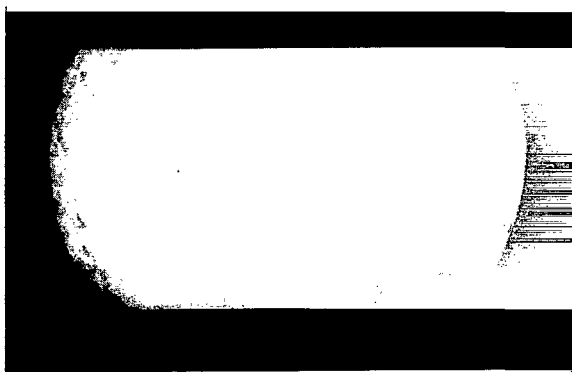


(7.28)

DISTANCE FROM IGNITOR (Cm)

MARKER	100
FLAME FRONT	96.6
SHOCK FRONT	96.6

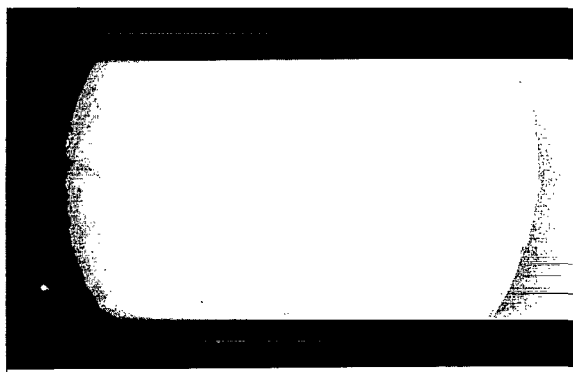
FIG. 7 (CONT'D) SHADOWGRAPHS OF THE FORMATION OF THE DETONATION WAVE; IGNITION AT END B.



(7.29)

DISTANCE FROM IGNITOR (Cm)

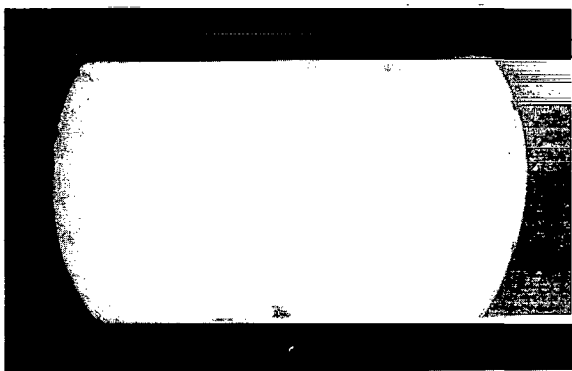
MARKER	100
FLAME FRONT	103.1
SHOCK FRONT	103.1



(7.30)

DISTANCE FROM IGNITOR (Cm)

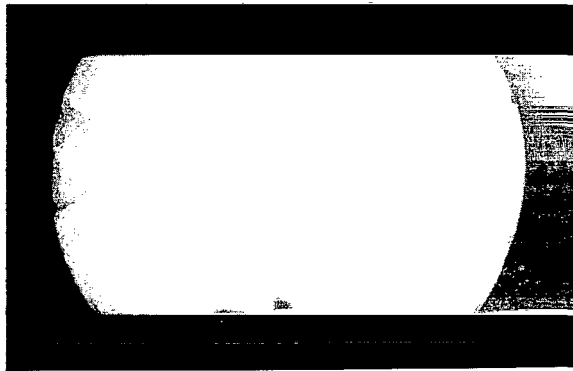
MARKER	108
FLAME FRONT	107.6
SHOCK FRONT	107.6



(7.31)

DISTANCE FROM IGNITOR (Cm)

MARKER	108
FLAME FRONT	109.3
SHOCK FRONT	109.3

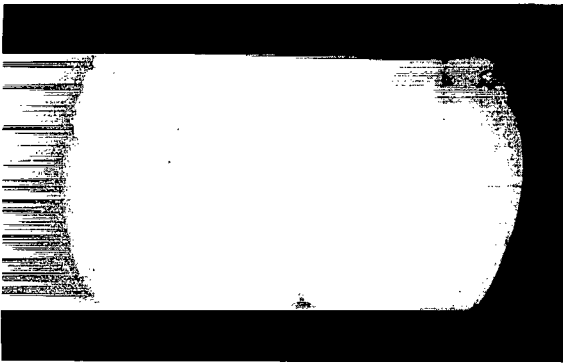


(7.32)

DISTANCE FROM IGNITOR (Cm)

MARKER	108
FLAME FRONT	NOT IN VIEW
SHOCK FRONT	NOT IN VIEW

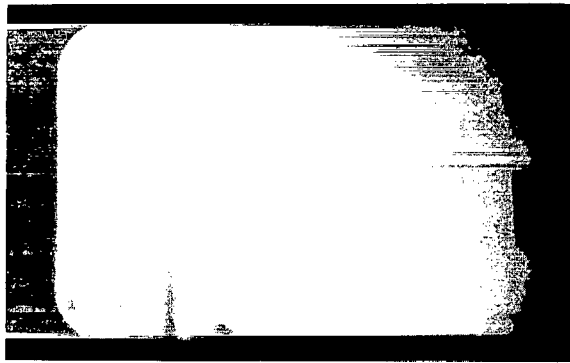
FIG. 7 (CONT'D) SHADOWGRAPHS OF THE FORMATION OF THE DETONATION WAVE; IGNITION AT END B.



(7.33)

DISTANCE FROM IGNITOR (Cm)

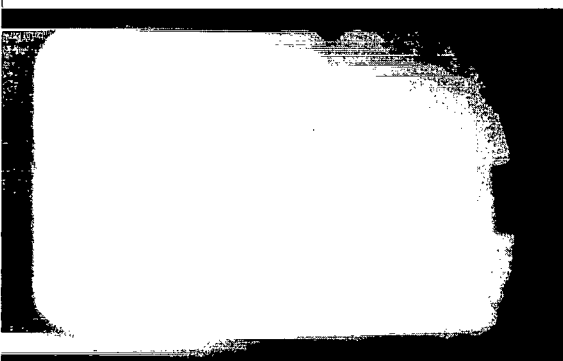
MARKER	116
FLAME FRONT	119.6
SHOCK FRONT	119.6



(7.34)

DISTANCE FROM IGNITOR (Cm)

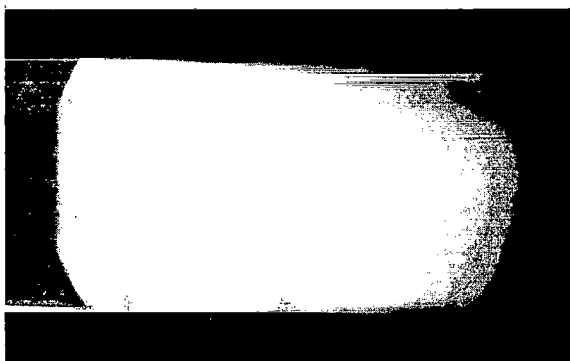
MARKER	124
FLAME FRONT	122.2
SHOCK FRONT	123.1



(7.35)

DISTANCE FROM IGNITOR (Cm)

MARKER	124
FLAME FRONT	128.5
SHOCK FRONT	128.5

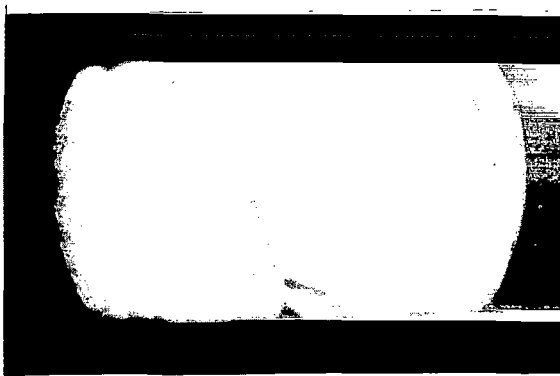


(7.36)

DISTANCE FROM IGNITOR (Cm)

MARKER	132
FLAME FRONT	128
SHOCK FRONT	128

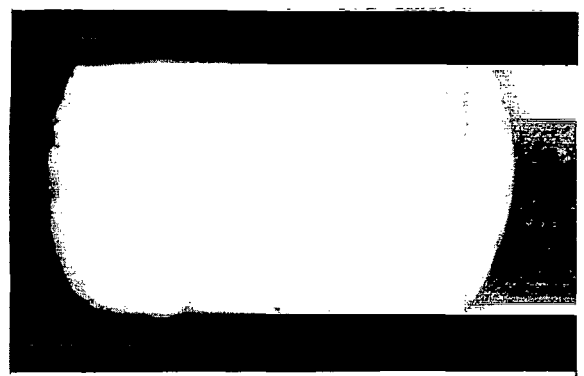
FIG. 7 (CONT'D) SHADOWGRAPHS OF THE FORMATION OF THE DETONATION WAVE; IGNITION AT END B.



(7.37)

DISTANCE FROM IGNITOR (Cm)

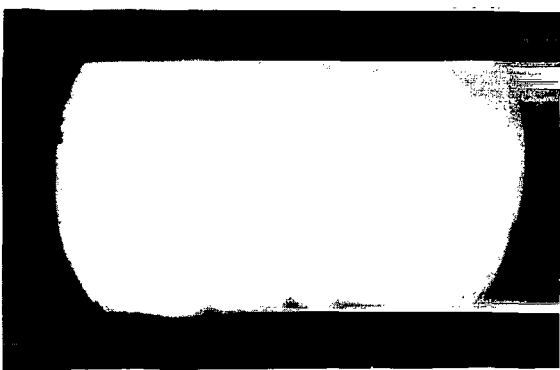
MARKER	132
FLAME FRONT	134.5
SHOCK FRONT	UNKNOWN



(7.38)

DISTANCE FROM IGNITOR (Cm)

MARKER	140
FLAME FRONT	138
SHOCK FRONT	138



(7.39)

DISTANCE FROM IGNITOR (Cm)

MARKER	140
FLAME FRONT	137.7
SHOCK FRONT	137.7

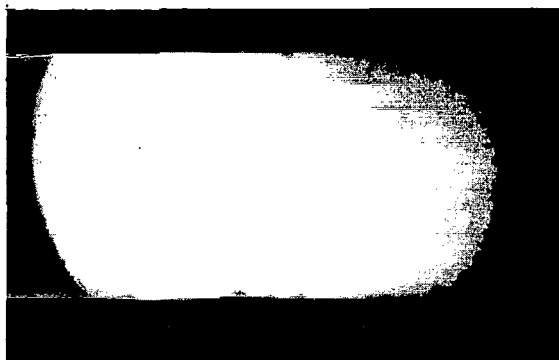


(7.40)

DISTANCE FROM IGNITOR (Cm)

MARKER	140
FLAME FRONT	142.5
SHOCK FRONT	142.5

FIG. 7 (CONT'D) SHADOWGRAPHS OF THE FORMATION OF THE DETONATION WAVE; IGNITION AT END B.



(7.41)

DISTANCE FROM IGNITOR (Cm)

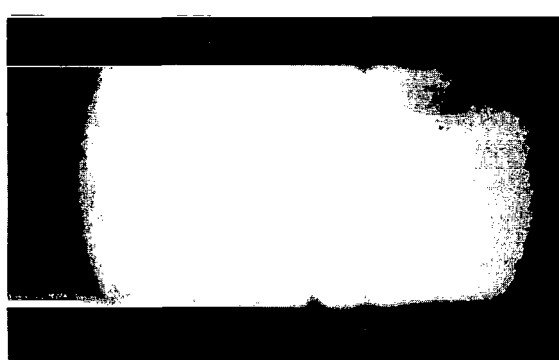
MARKER	148
FLAME FRONT	148
SHOCK FRONT	148



(7.42)

DISTANCE FROM IGNITOR (Cm)

MARKER	148
FLAME FRONT	149.8
SHOCK FRONT	149.8



(7.43)

DISTANCE FROM IGNITOR (Cm)

MARKER	156
FLAME FRONT	157.8
SHOCK FRONT	157.8

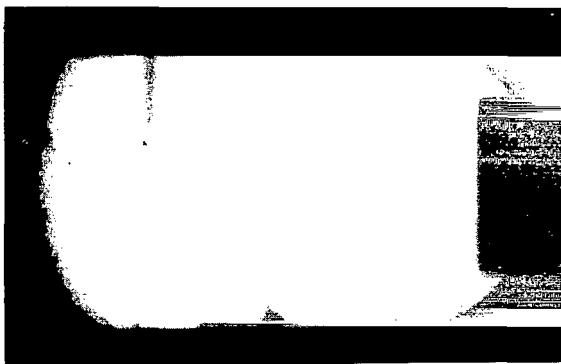


(7.44)

DISTANCE FROM IGNITOR (Cm)

MARKER	156
FLAME FRONT	161
SHOCK FRONT	161

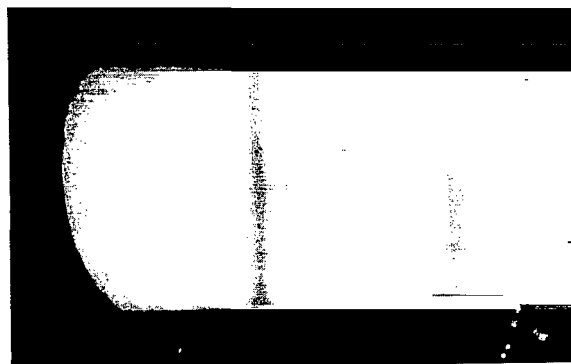
FIG. 7 (CONT'D) SHADOWGRAPHS OF THE FORMATION OF THE DETONATION WAVE; IGNITION AT END B.



(7.45)

DISTANCE FROM IGNITOR (Cm)

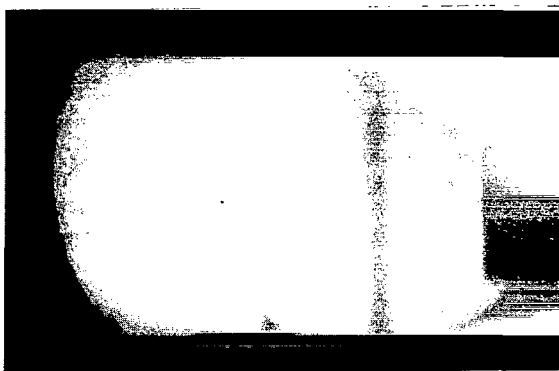
MARKER	159.5
FLAME FRONT	156.1
SHOCK FRONT	156.1



(7.46)

DISTANCE FROM IGNITOR (Cm)

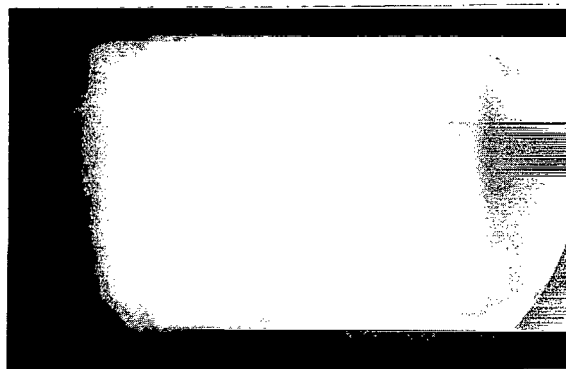
MARKER	159.5
FLAME FRONT	159.5
SHOCK FRONT	159.5



(7.47)

DISTANCE FROM IGNITOR (Cm)

MARKER	159.5
FLAME FRONT	162.7
SHOCK FRONT	162.7



(7.48)

DISTANCE FROM IGNITOR (Cm)

MARKER	159.5
FLAME FRONT	UNKNOWN
SHOCK FRONT	156.5

FIG. 7 (CONT'D) SHADOWGRAPHS OF THE FORMATION OF THE DETONATION WAVE; IGNITION AT END B.

2/7/25
e

"The National Aeronautics and Space Administration . . . shall . . . provide for the widest practical appropriate dissemination of information concerning its activities and the results thereof . . . objectives being the expansion of human knowledge of phenomena in the atmosphere and space."

—NATIONAL AERONAUTICS AND SPACE ACT OF 1958

NASA SCIENTIFIC AND TECHNICAL PUBLICATIONS

TECHNICAL REPORTS: Scientific and technical information considered important, complete, and a lasting contribution to existing knowledge.

TECHNICAL NOTES: Information less broad in scope but nevertheless of importance as a contribution to existing knowledge.

TECHNICAL MEMORANDUMS: Information receiving limited distribution because of preliminary data, security classification, or other reasons.

CONTRACTOR REPORTS: Technical information generated in connection with a NASA contract or grant and released under NASA auspices.

TECHNICAL TRANSLATIONS: Information published in a foreign language considered to merit NASA distribution in English.

TECHNICAL REPRINTS: Information derived from NASA activities and initially published in the form of journal articles or meeting papers.

SPECIAL PUBLICATIONS: Information derived from or of value to NASA activities but not necessarily reporting the results of individual NASA-programmed scientific efforts. Publications include conference proceedings, monographs, data compilations, handbooks, sourcebooks, and special bibliographies.

Details on the availability of these publications may be obtained from:

SCIENTIFIC AND TECHNICAL INFORMATION DIVISION
NATIONAL AERONAUTICS AND SPACE ADMINISTRATION

Washington, D.C. 20546